Chapter 3
Probabilities of Radiative Transitions

Abstract In this chapter, we consider the probability of photoprocesses including bound–bound, bound–free, and free–free electronic transitions. This concerns atomic radiation transitions in the discrete energy spectrum, radiative recombination, Bremsstrahlung including polarization channel, photoionization, photodetachment of negative ions, and phase control of photoprocesses by ultrashort laser pulses. Considerable attention has been paid to various types of broadening of the spectral lines of atomic radiative transitions, including plasma broadening mechanisms. The rotational approximation of the Kramers electrodynamics is presented which is suitable for describing both free–free and free–bound electronic transitions in the high frequency limit. The photoionization of atoms is described both within the framework of a rigorous quantum mechanical approach and with the help of a number of approximate methods. Analytical generalized photoionization cross section formulas from K-, L-, M-, N-, and O-shell that include also possible inner-shell photoionization are presented. Finally, generalized scaled formulas for radiation recombination rates into all states with principal quantum numbers n = 1–9 and orbital quantum numbers l = 0–8 are given that can be applied for a large variety of practical cases.

3.1 Radiative Transition Cross Sections

To calculate the probability per unit time (rate) for a phototransition between atomic energy levels, together with the Einstein coefficient for an induced process (2.29), a radiative transition cross section is widely used. In a monochromatic field of frequency ω it is determined by the equation

$$\sigma_{\mathrm{jn}}(\omega) = \frac{w_{\mathrm{jn}}}{j(\omega)}, \tag{3.1}$$

F. B. Rosmej et al., *Plasma Atomic Physics*, Springer Series on Atomic, Optical, and Plasma Physics 104, https://doi.org/10.1007/978-3-030-05968-2_3

where

$$j(\omega) = \frac{cE_0^2}{8\pi\hbar\omega} \tag{3.2}$$

is the photon flux density at a specified frequency and E_0 is the amplitude of the strength of the electric field of monochromatic radiation. Since the dimensionality of the probability per unit time w_{jn} is $[s^{-1}]$ and the dimensionality of the photon flux density is $[s^{-1}m^{-2}]$, it follows from (3.1) that the cross section has the dimensionality $[m^2]$, i.e., the dimensionality of an area. Thus, we can say that the cross section describes some effective area of a hard sphere: If the projectile trajectory touches the hard sphere, a transition takes place, and if the trajectory lies outside, no transition occurs.

Using the formulas (2.28), (2.30), we find from (3.1) to (3.2) the following expression for the cross section of the transition $n \to j$:

$$\sigma_{jn}(\omega) = \frac{2\pi^2 e^2}{mc} f_{jn} G_{jn}^{(h)}(\omega), \tag{3.3}$$

where $G_{jn}^{(h)}(\omega)$ is the spectral form of a line of the homogeneously broadened transition, and f_{jn} is the transition oscillator strength (2.18). From the expression (3.3), it follows in particular that a large oscillator strength implies a large cross section. For dipole-forbidden transitions, when $f_{jn} = 0$, the cross section is equal to zero.

Substituting the expression for the oscillator strength (2.18) into (3.3), we obtain the expression for the phototransition cross section in terms of the matrix element of the dipole moment $\boldsymbol{d}_{jn}$:

$$\sigma_{jn}(\omega) = \frac{4\pi^2 \omega_{jn}}{3\hbar c g_n} |\langle n|\boldsymbol{d}|j\rangle|^2 G_{jn}^{(h)}(\omega). \tag{3.4}$$

g_n is the statistical weight (the degeneracy factor) of a nth atomic energy level. Because $G_{jn}^{(h)}(\omega)$ has it maximum value at $\omega = \omega_{jn}$, the maximum value of the cross section corresponds to the frequency $\omega = \omega_{jn}$ (the resonance condition):

$$\sigma_{jn}^{(\max)} = \sigma_{jn}(\omega = \omega_{jn}) = \frac{8\pi}{3\hbar c g_n} |\langle n|\boldsymbol{d}|j\rangle|^2 \frac{\omega_{jn}}{\Delta\omega_{jn}}, \tag{3.5}$$

that is, it is proportional to the ratio of the eigenfrequency to the spectral characteristic width of an atomic transition line. This ratio is similar to the resonator Q-factor and is equal to the number of free oscillations of the oscillator until their total damping. It should be noted that in the early works of M. Planck and A. Einstein on the quantum theory of electromagnetic interaction atoms and molecules of a substance were called resonators.

In case of natural broadening, when $\Delta\omega_{jn} = A_{nj}$, (3.5) is transformed with (2.26) to the form:

$$\sigma_{jn}^{(max)} = \frac{g_j}{2\pi g_n}\lambda_{jn}^2. \tag{3.6}$$

Hence, it follows that the resonance cross section of a phototransition in case of natural broadening of a line is proportional to the squared of the resonant wavelength $\lambda_{jn} = 2\pi c/\omega_{jn}$; that is, in a wide spectral range, it exceeds by many orders of magnitude the geometrical cross section of an atom (equal to its area). It should be noted that the maximum cross section does not depend on the matrix element of the dipole moment.

For an atom under the action of radiation with a finite spectral width $\Delta\omega \neq 0$, the probability per unit time for the excitation of an atomic transition $n \to j$ is given by the integral

$$w_{jn} = \int \sigma_{jn}(\omega')j(\omega')\mathrm{d}\omega'. \tag{3.7}$$

If the radiation spectrum considerably exceeds the spectral width of the transition line, i.e. $\Delta\omega \gg \Delta\omega_{jn}$, as it is the case, for example, for the thermal radiation, the spectral form of a transition line in the definition of the cross section can be replaced by the delta function $G_{jn}^{(h)}(\omega') \to \delta(\omega' - \omega_{jn})$, and the integral (3.7) gives:

$$w_{jn} = \frac{4\pi^2\omega_{jn}}{3\hbar c g_n}|\langle n|\boldsymbol{d}|j\rangle|^2 j(\omega_{jn}) = B_{jn}\rho(\omega_{jn}) \tag{3.8}$$

since $j(\omega) = c\rho(\omega)/\hbar\omega$, $\rho(\omega)$ is the spectral radiation density. The second equality in formula (3.8) coincides with the relation that was used by A. Einstein to describe the interaction of thermal radiation with a two-level atom.

In the general case of an arbitrary relation between the widths of radiation spectra and the atomic transition in an atom, the expression (3.7) should be used for the calculation of the photoexcitation rate. It should be noted that for the calculation of the probability per unit time for a phototransition, instead of a cross section, the concept of a spectral Einstein coefficient

$$D_{jn}(\omega) = B_{jn}G_{jn}(\omega) \tag{3.9}$$

is sometimes used. The formula (3.7) can be rewritten in terms of the spectral Einstein coefficient (3.9) with replacement of the photon flux density $j(\omega)$ by the spectral radiation energy density $\rho(\omega)$.

The atomic transition $n \to j$ induced by the action of radiation corresponds to photon absorption, if $E_n < E_j$. The reverse transition $j \to n$ corresponds to photon radiation that can be both induced (under the action of an external field) and spontaneous. The cross section of induced radiation $\sigma_{nj}(\omega)$ is described by formulas

similar to (3.3)–(3.4) because the matrix element of the dipole moment can be made symmetric by selection of the wave functions, i.e. $\langle n|\boldsymbol{d}|j\rangle = \langle j|\boldsymbol{d}|n\rangle$ and $G_{\mathrm{jn}}^{(h)}(\omega) = G_{\mathrm{nj}}^{(h)}(\omega)$ and the difference in expressions for the cross sections of induced radiation and absorption consists only in different statistical weights of states. Therefore, the expression for the cross section of induced radiation $\sigma_{\mathrm{nj}}(\omega)$ for the transition $j \to n$ is obtained from (3.4) by the replacement $g_{\mathrm{n}} \to g_{\mathrm{j}}$.

It is easy to express the absorption coefficient k_{jn} in terms of the absorption cross section in order to describe electromagnetic wave damping in the propagation in a medium with resonant atoms. The damping is a result of a transition in an atom from a lower to a higher energy state, i.e. $n \to j$ ($E_{\mathrm{n}} < E_{\mathrm{j}}$): $k_{\mathrm{jn}} = N_{\mathrm{n}}\sigma_{\mathrm{jn}}$, where N_{n} is the concentration of atoms in the state n. It is obvious that the absorption coefficient has the dimensionality of reciprocal length [m^{-1}]. By analogy with the absorption coefficient, it is possible to introduce an amplification coefficient for the reverse transition $j \to n$ corresponding to induced radiation of a photon and an increase in radiation intensity: $k_{\mathrm{nj}} = N_{\mathrm{j}}\sigma_{\mathrm{nj}}$. Therefore, the effective amplification coefficient taking into account induced radiation and absorption can be expressed as follows:

$$k_{\mathrm{nj}}^{(\mathrm{tot})} = k_{\mathrm{nj}} - k_{\mathrm{jn}} = g_{\mathrm{j}}\sigma_{\mathrm{nj}}(\omega)\left\{\frac{N_{\mathrm{j}}}{g_{\mathrm{j}}} - \frac{N_{\mathrm{n}}}{g_{\mathrm{n}}}\right\}. \tag{3.10}$$

If $k_{\mathrm{nj}}^{(\mathrm{tot})} > 0$ (induced radiation dominates), radiation is amplified by the medium of resonant atoms. Otherwise radiation is attenuated since photon absorption dominates over induced radiation. Since the atomic transition cross section is a positive number, then, as follows from the formula (3.10), amplification of radiation is given by the condition:

$$\frac{N_{\mathrm{j}}}{g_{\mathrm{j}}} - \frac{N_{\mathrm{n}}}{g_{\mathrm{n}}} > 0, \quad E_{\mathrm{n}} < E_{\mathrm{j}}. \tag{3.11}$$

The relation (3.11) is called the *population inversion* condition. It is widely used in quantum electronics, laser physics, and analogous to the study of possible radiation amplification. In thermodynamic equilibrium, when the Boltzmann formula for energy level populations holds true, an inequality reverse to (3.11) is fulfilled. Thus, to obtain population inversion, it is necessary to disturb a substance considerably from its thermal equilibrium state. This is usually achieved by the action of external photons on a medium being called pumping.

The concept of a cross section is used not only for the description of absorption and induced radiation, but it also characterizes other photoinduced processes such as photon scattering, photorecombination, and bremsstrahlung. The cross section concept is likewise used in calculations of the interaction of other elementary particles (electrons, protons, neutrons) with atoms and molecules. In all cases, the cross section is determined by a formula similar to (3.1), with replacement of the photon flux density by the flux density of particles that induce the process under consideration.

It should be noted that the concept of probability per unit time for a photoinduced process loses its physical meaning for ultrashort electromagnetic pulses where the duration of radiation is of the order of the period of the electric field oscillations at the carrier frequency. Ultrashort pulses can be produced with the use of special methods of time compression of laser radiation (CPA: chirped pulse amplification). To ultrashort pulses in the optical range there corresponds a duration of several femtoseconds. At present, in the visible range of laser wavelengths of well-controlled shapes with durations of only 1.5 periods of the optical frequency have been produced. In the UV range, pulse durations down to several hundreds of attoseconds have been achieved. To describe the interaction of ultrashort radiation pulses with a substance, it is more adequate to use the concept of the total probability for a process (i.e., during the total action of a pulse) that can be expressed in terms of a cross section (Rosmej et al. 2014, 2016, 2021).

3.2 Spectral Line Shapes of Atomic Radiative Transitions

The relations (2.28)–(2.29) were obtained in the limit of radiation with a broad spectrum (the so-called broadband illumination). In the general case, using the same approach as for the derivation of (2.37), it is possible [using (2.27)] to find the following expression for absorbed power by the transition $n \to j$:

$$P_{\mathrm{jn}} = \frac{2\pi^2 e^2}{3m} f_{\mathrm{jn}} \int_0^\infty G_{\mathrm{jn}}^{(h)}(\omega')\rho(\omega')\mathrm{d}\omega', \tag{3.12}$$

where

$$G_{\mathrm{jn}}^{(h)}(\omega') = \frac{\left(\delta_{\mathrm{jn}}/\pi\right)}{\left(\omega_{\mathrm{jn}} - \omega'\right)^2 + \left(\delta_{\mathrm{jn}}\right)^2} \tag{3.13}$$

is the spectral form (profile) of a line transition in case of homogeneous broadening. The function (3.13) is called the Lorentz function or Lorentzian. From (3.12) to (3.13), it follows that external field frequencies are most effectively absorbed in the vicinity of the transition eigenfrequency ω_{jn}. The characteristic frequency interval, in which the interaction between radiation and the atom is most intensive, is given by the damping constant: $\left|\omega_{\mathrm{jn}} - \omega'\right| \le \delta_{\mathrm{jn}}$. Hence, it follows that a characteristic width of an atomic transition line (in view of both detuning signs) is given by $\Delta\omega_{\mathrm{jn}}^{(h)} = 2\delta_{\mathrm{jn}}$. Substituting the damping constant from the last equation into (3.13), we obtain the form of a line of a homogeneously broadened transition in an atom or in any other quantum system.

Instead of the characteristic width $\Delta\omega_{\mathrm{jn}}^{(h)}$, a characteristic time can be introduced according to

$$T_2 = \frac{2}{\Delta\omega_{\mathrm{jn}}^{(h)}}. \tag{3.14}$$

The parameter T_2 is called the transverse relaxation time or the phase relaxation time. It is related to the damping constant of a transition oscillator according to $T_2 = 1/\delta_{\mathrm{jn}}$ and therefore, as it follows from (3.14), defines the lifetime of a transition oscillator in the mode of free oscillation. The time T_2 (as will be shown below) is called the *irreversible* phase relaxation time.

Thus, from the point of view of the spectroscopic principle of correspondence, homogeneous broadening of a spectral line is defined by the damping of a transition oscillator occurring in free oscillation without external field.

An important particular case of homogeneous broadening is *natural broadening* of a line due to spontaneous radiation: $\Delta\omega_{\mathrm{jn}}^{(h)} = A_{\mathrm{nj}}$. In this case, transition oscillator damping is caused by the interaction of an atomic electron with the vacuum fluctuations of an electromagnetic field. Natural broadening for an atom in free space is the minimum possible, and it defines the degree of radiation monochromaticity that is in principle achievable.

Another type of broadening occurs in interaction of radiation with an ensemble of atoms when the transition eigenfrequency is spread over $\Delta\omega_{\mathrm{jn}}^{(\mathrm{inh})}$ for different atoms. This means that every atom has a specific frequency shift and the observed frequency spread belongs to the ensemble of atoms. This spread defines *inhomogeneous broadening* of a line. The spectral form (shape) is determined by the distribution function of the frequency shifts. In the case of a Gaussian distribution function, one has (Gaussian):

$$G_{\mathrm{jn}}^{(\mathrm{inh})}(\omega') = \frac{1}{\sqrt{2\pi}\Delta\omega_{\mathrm{jn}}^{(\mathrm{inh})}} \exp\left\{ -\frac{\left(\omega' - \omega_{\mathrm{jn}}^{(c)}\right)^2}{2\left(\Delta\omega_{\mathrm{jn}}^{(\mathrm{inh})}\right)^2} \right\}, \tag{3.15}$$

where $\omega_{\mathrm{jn}}^{(c)}$ is the central frequency of a transition in an ensemble of atoms.

The spectral forms of lines for homogeneous (Lorentzian) and inhomogeneous (Gaussian) broadening are presented in Fig. 3.1 for $\omega_{\mathrm{jn}}^{(c)} = \omega_{\mathrm{jn}}$ and $\Delta\omega_{\mathrm{jn}}^{(\mathrm{inh})} = \Delta\omega_{\mathrm{jn}}^{(h)}$; the coordinate axes are plotted in relative units, i.e. $(\omega' - \omega_{\mathrm{jn}}^{(c)})/\Delta\omega_{\mathrm{jn}}^{(\mathrm{inh})}$.

It is seen that the spectral form of a homogeneous broadened line has more extended "wings" compared to inhomogeneous Gaussian broadening. The functions (3.13), (3.15) have two common properties: (1) normalization to unity and (2) both functions tend to the Dirac delta function in the limit of zero width.

Different causes can produce inhomogeneous broadening of a line depending on the concrete realization of the radiative transition. For atoms in a gas and ions in

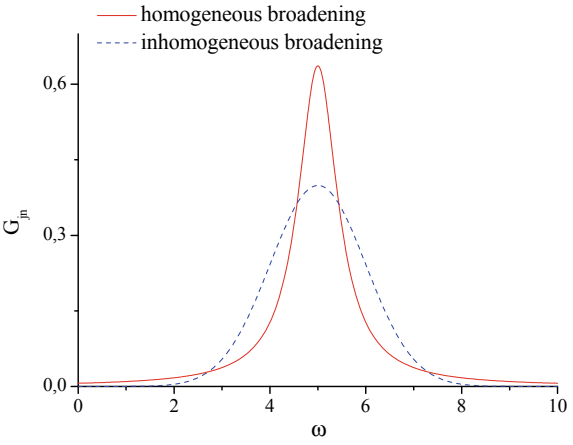

Fig. 3.1 Homogeneous and inhomogeneous broadening of a spectral line

a plasma, an important mechanism of inhomogeneous broadening is the Doppler effect. According to this effect, the radiation frequency from the intrinsic frame of reference is connected with an atom in the laboratory frame of reference by the formula

$$\omega = \gamma\omega_0\left(1 - \frac{\upsilon}{c}\cos\theta\right) \equiv \gamma\omega_0\left(1 - \frac{\upsilon_k}{c}\right), \tag{3.16}$$

where ω_0 is the frequency in the frame of reference of the radiating atom, $\gamma = \left(1 - (\upsilon/c)^2\right)^{-1/2}$ is the Lorentz factor, θ is the angle between the atomic velocity vector and the photon wave vector (the angle of radiation), and υ_k is the projection of the atomic (ionic) velocity on the direction of photon radiation. In gases and low-temperature plasmas $\upsilon \ll c$ and $\gamma \cong 1$. Since the velocity of atoms/ions in thermal equilibrium has a distribution, the width that is defined by the thermal velocity $\upsilon_T = \sqrt{2T/M}$ (M is the mass of an atom/ion) and the radiation frequency in the laboratory frame of reference [see (3.16)] will also have a distribution. The Doppler profile can be represented in terms of the integral

$$G_{ki}^{(D)}(\omega) = \int_{-\infty}^{\infty} \delta\left(\omega - \omega_{ki}\left(1 - \frac{\upsilon_k}{c}\right)\right) f(\upsilon_k)\mathrm{d}\upsilon_k, \tag{3.17}$$

where $f(\upsilon_k)$ is the function of distribution of atomic (ionic) velocity projections on a specified direction. The delta function in the right-hand side of (3.17) marks out those values of velocity projections, at which, according to the Doppler effect (3.16), the frequency in the laboratory frame of reference is equal to a specific value ω. The formula (3.17) corresponds to an interpretation of inhomogeneous broadening as a distribution function of atomic eigenfrequencies. We can say that the Doppler effect

maps the velocity distribution of atoms onto their eigenfrequency distribution. It should be noted that using the second equality in the right-hand side of (3.16) considerably simplifies the derivation of the expression for the Doppler profile.

In case of a Maxwellian velocity distribution, i.e.

$$f(\upsilon_k) = \frac{1}{\sqrt{\pi}\upsilon_T} \exp\left(-\left(\frac{\upsilon_k}{\upsilon_T}\right)^2\right), \tag{3.18}$$

the calculation of the integral (3.17) gives

$$G_{ki}^{(D)}(\omega) = \frac{1}{\sqrt{2\pi}\Delta\omega_{ki}^{(D)}} \exp\left[-\frac{(\omega-\omega_{ki})^2}{2\left(\Delta\omega_{ki}^{(D)}\right)^2}\right], \tag{3.19}$$

where

$$\Delta\omega_{ki}^{(D)} = \frac{1}{\sqrt{2}}\frac{\upsilon_T}{c}\omega_{ki} \equiv \sqrt{\frac{T}{M}}\frac{\omega_{ki}}{c} \tag{3.20}$$

is the Doppler line width (note that the FWHM is given by $2\sqrt{\ln 2}\cdot\Delta\omega_{ki}^{(D)}$; see also (1.22)).

The right-hand side of (3.20) includes a temperature defining the translational velocity of atoms (ions) in the plasma and is called the ion temperature. As can be seen from (3.20), the measurement of the Doppler line width for radiation with a specified central frequency allows determining the ion temperature of the plasma if the mass of the radiating atom (ion) is known. According to the formula (3.20), the Doppler line width is proportional to the central radiation frequency, so the role of the Doppler effect increases with energy of an atomic transition. For the optical range and room temperatures, Doppler broadening is of the order of 10 GHz.

A Doppler profile being of the form (3.19) assumes an unchanged velocity of the atom during radiation emission. This condition is realized if the free path of an atom/ion in a gas or a plasma is larger than the wavelength of the radiation. However, it can be violated for sufficiently dense and hot plasmas such as laser-produced plasmas. Then, the line profile is close to be a Lorentz profile (3.13), with a line width that is inversely proportional to the atomic collision frequency. In rarefied low-temperature plasmas, the line profile is described by the formula (3.19).

Another mechanism of inhomogeneous line broadening characteristic to atoms/ions in plasma is connected with the Stark effect (Griem 1974, 1997; Sobelman et al. 1995). The Stark effect represents a shift (and, generally speaking, splitting) of the spectral line radiation of an atom under the action of an external electric field. Inhomogeneous broadening under the action of the Stark effect occurs in case of a static (or sufficiently slowly varying with time) electric field. Such fields are

produced by plasma ions due to relatively low (in comparison with electrons) velocity (because the mass of ions is much larger than the electron mass). The expression for the Stark effect that is linear with respect to the electric field looks like

$$\omega - \omega_{\mathrm{ik}} = C_{\mathrm{ik}} F, \tag{3.21}$$

where F is the magnitude of the electric field strength at the location of an atom (ion) and C_{ik} is the Stark constant for the atomic transition. The linear Stark effect is characteristic for hydrogen-like ions where we encounter degeneracy in orbital quantum number.

Let us consider the influence of the Stark effect on the form of a spectral line in the static case when the electric field that acts on the radiating atom is a result of a large number of plasma ions. Then for the strength of the total electric field, we have

$$\boldsymbol{F} = \sum_{\mathrm{j}=1}^{N_0} \boldsymbol{F}_{\mathrm{j}} = \sum_{\mathrm{j}=1}^{N_0} e \frac{\boldsymbol{r}_{\mathrm{j}}}{r_{\mathrm{j}}^3}, \tag{3.22}$$

where the summation is carried out over all plasma ions, with N_0 being the number of ions. For simplicity, we assumed $Z = 1$ in (3.22). The relation (3.21) establishes a univocal correspondence between the electric field and the frequency shift. Therefore, if the distribution function for the electric field strength $W(\boldsymbol{F})$ is known, it is easy to find with the help of the formula (3.21) the frequency distribution function that is a line profile for inhomogeneous broadening. This function looks like

$$G_{\mathrm{ik}}^{(\mathrm{St})}(\omega) = \frac{1}{C_{\mathrm{ik}}} W\left(\frac{\omega - \omega_{\mathrm{ik}}}{C_{\mathrm{ik}}}\right). \tag{3.23}$$

The factor in front of the ion field distribution function results from the relation $\mathrm{d}F/\mathrm{d}\omega = 1/C_{\mathrm{ik}}$ being the frequency transformation of the field distribution.

Thus, a key problem is the determination of the ion field distribution function $W(\boldsymbol{F})$. Following Holtsmark, simple expressions can be obtained in the approximation of negligible correlation between the plasma ions. Then, the probability for ions having a radius vector in the interval $(\boldsymbol{r}_{\mathrm{j}}, \boldsymbol{r}_{\mathrm{j}} + \mathrm{d}\boldsymbol{r}_{\mathrm{j}})$ is proportional to the product $V^{-N_0} \prod_{\mathrm{j}=1}^{N_0} \mathrm{d}\boldsymbol{r}_{\mathrm{j}}$, where V is the plasma volume. The probability $W(\boldsymbol{F})$ is proportional to that part of the N_0-dimensional space in variables $\boldsymbol{r}_{\mathrm{j}}$, in which (3.22) is fulfilled. According to this, the formula for the ion field distribution function is given by:

$$W(\boldsymbol{F}) = \left\langle \delta\left(\boldsymbol{F} - \sum_{\mathrm{j}=1}^{N_0} e \frac{\boldsymbol{r}_{\mathrm{j}}}{r_{\mathrm{j}}^3}\right) \right\rangle, \tag{3.24}$$

where averaging is done over the above distribution of ion radii. The explicit form of the function $W(\boldsymbol{F})$ can be obtained when using the integral representation of the delta function and going to the limit $N_0,\ V \to \infty$ at constant concentration of the ions $N = N_0/V$. As a result, the following expression is obtained (Unsöld 1955):

$$W(\boldsymbol{F})\mathrm{d}\boldsymbol{F} = W(F)\mathrm{d}F = H\left(\frac{F}{F_0}\right)\frac{\mathrm{d}F}{F_0}, \tag{3.25}$$

where

$$H(\beta) = \frac{2}{\pi}\beta\int_0^\infty x\sin(\beta x)\exp\left(-x^{3/2}\right)\mathrm{d}x \tag{3.26}$$

is the so-called Holtsmark distribution, $\beta = F/F_0$, $F_0 = \alpha e N^{2/3}$ is a scaling factor of the electric field strength and $\alpha = 2\,\pi(4/15)^{2/3} \cong 2.603$. From (3.25), it follows that the ion field distribution depends only on the field strength. The plot of the Holtsmark function is presented in Fig. 3.2. The maximum of this function corresponds to a value $\beta = 1.607$.

The Holtsmark distribution function is normalized according to $\int_0^\infty H(\beta)\mathrm{d}\beta = 1$. In the vicinity of zero, $H(\beta)$ increases as β^2, and at $\beta \gg 1$ it decreases as $\beta^{-5/2}$. The Holtsmark distribution differs essentially from the Gaussian distribution (3.15) that describes spectral line broadening as a result of the Doppler effect. It is close to the Gaussian velocity distribution for low $\beta \ll 1$, when the contribution to the field originates from a large number of ions. As is known, statistical regularities in ensembles of particles are described just by the Gaussian distribution. For strong fields, the Holtsmark distribution coincides with the distribution of a field from one nearest particle (the binary approximation). Thus, the Holtsmark function describes the transition from the Gaussian distribution for weak fields to the binary

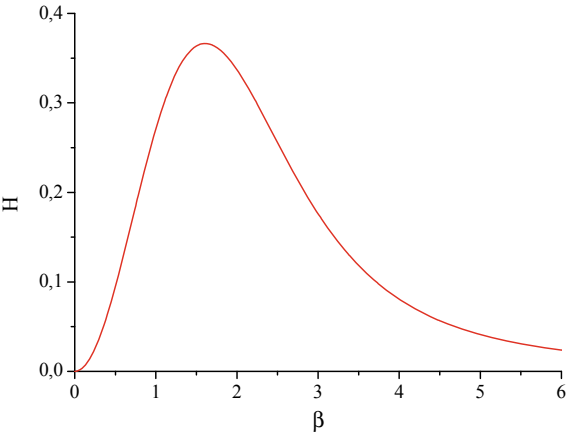

Fig. 3.2 Holtsmark function according to (3.26)

distribution for strong fields. Curiously, the scaled field strength of the Holtsmark distribution $F_0 = 2.603\, eN^{2/3}$ differs from the field at an average interionic distance $\bar{F} = e(4\pi N/3)^{2/3} \approx 2.61\, eN^{2/3}$ by less than one percent.

In plasma, a change of the phase of a transition oscillator (an equivalent oscillator) leading to homogeneous broadening can be a result from a collision between an atom and a charged particle. Let us consider this process for the case of interaction of electrons with a hydrogen-like atom. Then, an instantaneous change of the oscillator frequency $\omega(t)$ under the action of the electric field $F(t)$ of a plasma electron can be represented as

$$\omega(t) = \frac{C}{e} F(t), \tag{3.27}$$

where C is the Stark constant. The change of the phase of an equivalent oscillator during the time of electron transit close to the atom (ion) is given by

$$\Delta\phi = \int_{-\infty}^{\infty} \omega(t)\mathrm{d}t = \int_{-\infty}^{\infty} \frac{C}{\rho^2 + \upsilon^2 t^2}\mathrm{d}t = \pi \frac{C}{\rho\upsilon}, \tag{3.28}$$

ρ is the impact parameter, υ is the velocity of the perturbing particle assumed to be moving uniformly on a straight trajectory. From (3.28), it follows that a phase change $\Delta\varphi = \pi$ is achieved at

$$\rho_{\mathrm{W}} = \frac{C}{\upsilon}. \tag{3.29}$$

This value is called the Weisskopf radius; it defines the region of impact parameters corresponding to an essential change of the equivalent oscillator phase. To the radius ρ_{W}, there is related the Weisskopf cross section

$$\sigma_{\mathrm{W}} = \pi \rho_{\mathrm{W}}^2 = \pi \frac{C^2}{\upsilon^2} \tag{3.30}$$

and the Weisskopf frequency

$$\Omega = \frac{\upsilon}{\rho_{\mathrm{W}}} = \frac{\upsilon^2}{C}. \tag{3.31}$$

The parameter ρ_{W} defines the effective volume of interaction of an atom with perturbing particles. If there is one particle in this volume, the binary interaction takes place. Otherwise many particles interact simultaneously with an atom (non-binarity).

The Weisskopf frequency (3.31) separates impact and static limits for the spectral line shape. The profile of a line broadened by collisions with electrons can be represented in the form

$$G(\Delta\omega) = \frac{1}{2\pi}\frac{\Delta\omega(\omega-\omega_{ik})}{(\omega-\omega_{ik})^2 + (\Delta\omega(\omega=\omega_{ik})/2)^2} \tag{3.32}$$

that would coincide with the Lorentz profile (3.13) if the line width $\Delta\omega$ in the numerator of the right-hand side of the (3.32) would be a constant value (as in the denominator). In fact, the line width in the numerator depends on frequency detuning. If this detuning is much less (in magnitude) than the Weisskopf frequency (the impact limit), it can be considered that $\Delta\omega(\omega-\omega_{ik}) = \Delta\omega(\omega=\omega_{ik})$, and the Lorentz profile of a line (3.13) is realized. In the impact case, interaction of a quantum system with a perturbing particle is of instantaneous nature. As a result, the phase of oscillations of a transition oscillator "jumps". A typical value of impact broadening in gas at normal pressure and room temperature is about 100 GHz, so in the optical range it far exceeds natural broadening of a line, that has characteristic values of 100 MHz.

In the opposite case $|\omega-\omega_{ik}| \gg \Omega$ (the far wing of a line), it is necessary to take into account the frequency dependence of the line width in formula (3.32). Then, static broadening is realized, and the line profile (in the binary approximation) looks like

$$G_{ik}^{(st)}(\omega) = \frac{2\pi N C^{3/2}}{|\omega-\omega_{ik}|^{5/2}}. \tag{3.33}$$

The dependence on frequency detuning in the right-hand side of (3.33) coincides with the result of the Holtsmark approximation in the strong field limit, when $H(\beta \gg 1) \propto \beta^{-5/2}$. As was already noted, this coincidence is connected with the fact that in the strong field limit the static Holtsmark distribution coincides with the distribution of a field from one particle nearest to an atom; that is, the binary approximation is valid.

The condition $|\omega-\omega_{ik}| \gg \Omega$ means that in the static limit the time of interaction (ρ_W/υ) should be much larger than the time of spectral line formation $(\approx 1/|\omega-\omega_{ik}|)$. In the impact limit, on the contrary, the time of formation of a line is long, and perturbation can be considered to be instantaneous.

The expression for a line broadening in the static limit and the binary approximation (3.33) was obtained for an interaction charge-dipole. In the general case, when the energy of interaction of "broadening particles" with an atom (ion) looks like $U(R) = C_n/R^n$ (R is the distance between particles), the line profile in the static limit is described by the expression

$$G_{ik}^{(st)}(\omega) = \frac{4\pi N (C_n/\hbar)^{3/n}}{n|\omega - \omega_{ik}|^{(n+3)/n}}. \tag{3.34}$$

The obtained expression is valid in the spectral range $|\omega - \omega_{ik}| \gg \Omega$. From the formula (3.34), it follows that the frequency dependence in the static wing of a line coincides with the Lorentz dependence (3.13) only for $n = 3$, that is, for dipole–dipole interaction.

3.3 Quasi-classical and Quantum Radiative Transition Probabilities

3.3.1 Kramers Electrodynamics

The foundations of radiation theory for a classically moving particle (electron) in a given potential $U(r)$ are described in numerous books on classical electrodynamics (Jackson 2007; Landau and Lifschitz 2003). In accordance with Gervids and Kogan (1975, 1991), Kogan and Kukushkin (1984), Kogan et al. (1992) we shall dwell on a number of classical spectral peculiarities connected with the attractive potential $U(r) = -|U(r)|$ playing an important role in the applicability of classical mechanics to atomic physics. The essence of the problem involves the situation when an emitting electron in an attractive field experiences an acceleration and may obtain a kinetic energy $W = E + |U(r)|$, that considerably exceeds its initial energy E at infinity. In this case, the classical nature of the electron motion is even preserved when the quantum energy $\hbar\omega$ emitted by the electron exceeds its initial energy E. This circumstance essentially expands the domain of applicability of the classical methods to atomic processes, including the inelastic domain $\hbar\omega \geq E$. Below, we will focus on the Coulomb field case playing an important role for the atomic processes in plasmas. Atomic potentials of more general type are investigated in (Kogan and Kukushkin 1984). The results of the following considerations will be used later in the quasi-classical approximation for radiation transitions probabilities.

Classical electrodynamics (CED) operates with an effective spectral radiation yield $dk(\omega)$, cross section $d\sigma(\omega)$ and energy $dE(\rho, \omega)$ emitted during the time of the collision with an impact parameter ρ in a frequency domain $d\omega$. These values are connected by the relation

$$\frac{dk(\omega)}{d\omega} = \hbar\omega \frac{d\sigma}{d\omega} = \int_0^\infty 2\pi\rho d\rho [dE(\rho, \omega)/d\omega]. \tag{3.35}$$

The spectral distribution of the emitted energy is defined by the Fourier coefficients $\dot{x}(\rho, \omega)$ and $\dot{y}(\rho, \omega)$ of the electron velocity components $\dot{x}(\rho, t)$ and $\dot{y}(\rho, t)$:

$$\frac{\mathrm{d}E(\rho,\omega)}{\mathrm{d}\omega}=\frac{e^2}{3\pi c^3}\omega^2\left[|\dot{x}(\rho,\omega)+i\ddot{y}(\rho,\omega)|^2+|\dot{x}(\rho,\omega)-i\ddot{y}(\rho,\omega)|^2\right]. \tag{3.36}$$

These Fourier components for a motion in a Coulomb field are expressed in terms of the Hankel functions $H_{i\nu}^{(1)}(i\nu\varepsilon)$ and their derivatives $H_{i\nu}^{(1)'}(i\nu\varepsilon)$:

$$\frac{\mathrm{d}E(\rho,\omega)}{\mathrm{d}\omega}=\frac{2\pi Z^2e^6\omega^2}{3m^2\upsilon^4c^3}f(\nu,\varepsilon), \tag{3.37}$$

$$f(\nu,\varepsilon)=\left\{\left[H_{i\nu}^{(1)'}(i\nu\varepsilon)\right]^2-\left(1-\frac{1}{\varepsilon^2}\right)\left[H_{i\nu}^{(1)}(i\nu\varepsilon)\right]^2\right\}. \tag{3.38}$$

Here, $\nu=\omega/\tilde{\omega}$ is a dimensionless frequency in units of the "classical" Coulomb frequency, $\tilde{\omega}=\upsilon/a=m\upsilon^3/Ze^2$ ($a=Ze^2/m\upsilon^2$ is the Coulomb length), $\varepsilon^2=1+\rho^2/a^2$ is the eccentricity of the hyperbolic trajectory (ρ is the impact parameter): parameters Ze, m, υ, and c are the standard designations for nuclear charge, mass, electron velocity, and the speed of light, respectively.

The function $f(\nu,\varepsilon)$ is well known (Landau and Lifschitz 2003) being the complete derivative of the function

$$g(\nu)=\frac{\pi\sqrt{3}}{4}i\nu H_{i\nu}^{(1)}(i\nu\varepsilon)H_{i\nu}^{(1)'}(i\nu\varepsilon), \tag{3.39}$$

that makes it possible to perform the integration over $\mathrm{d}\rho$ in (3.35) and to obtain the cross section

$$\mathrm{d}\sigma(\omega)=\frac{16\pi e^2\upsilon^2}{3\sqrt{3}\hbar c^3}a^2\frac{\mathrm{d}\nu}{\nu}g(\nu). \tag{3.40}$$

The function $g(\nu)$ is named the Gaunt factor. For large radiation frequencies $\omega/\tilde{\omega}\gg 1$, the factor $g(\nu)$ approaches unity, and the numerical factor before $g(\nu)$ in (3.40) is the so-called Kramers bremsstrahlung cross section.

The total (integral over ω) effective radiation k is expressed in terms of the total radiation energy loss $\Delta E(\rho)$ during the collision:

$$k=\int\hbar\omega\frac{\mathrm{d}\sigma}{\mathrm{d}\omega}\mathrm{d}\omega=\int_0^\infty 2\pi\rho\mathrm{d}\rho\Delta E(\rho). \tag{3.41}$$

The magnitude $\Delta E(\rho)$ may be expressed, in turn, with the help of a time integral from the square of electron acceleration $w(\rho,t)$:

$$\Delta E(\rho) = \frac{2e^2}{3c^3} \int\limits_{-\infty}^{\infty} [w(\rho, t)]^2 \mathrm{d}t. \tag{3.42}$$

For the central field, (3.42) is rewritten in the form

$$\Delta E(\rho) = \frac{4e^2}{3m^2c^3} \int\limits_{r_0(\rho)}^{\infty} \left(\frac{\mathrm{d}U}{\mathrm{d}r}\right)^2 \frac{\mathrm{d}r}{\upsilon_\mathrm{r}}, \tag{3.43}$$

$\upsilon_\mathrm{r}(\rho)$ is the radial velocity, and $r_0(\rho)$ is the classical turning point defined from the relation

$$1 = \frac{\rho^2}{r_0^2} - \frac{|U(r_0)|}{E}. \tag{3.44}$$

Let us write down the spectral distributions of the emitted energy in the domain of large and small frequencies. Following (Kogan and Kukushkin 1984; Gervids and Kogan 1991), let us use the normalized spectral functions being the ratio of the spectral distribution $\mathrm{d}E(\rho, \omega)$ to the total radiation $\Delta E(\rho)$

$v \ll 1, \rho \gg a$:

$$\frac{\mathrm{d}E(\rho, \omega)}{\Delta E(\rho)} = \frac{8}{\pi^2} \left\{ [sK_0(s)]^2 + [sK_1(s)]^2 \right\} \mathrm{d}s, \tag{3.45}$$

$$s = M\omega/2E;$$

$v \gg 1, \rho \ll a$:

$$\frac{\mathrm{d}E(\rho, \omega)}{\Delta E(\rho)} = \frac{12}{\pi^2} G(u) u \mathrm{d}u, \tag{3.46}$$

$$u = M^3\omega/3Z^2me^4, \; G(u) = u\left[K_{1/3}^2(u) + K_{2/3}^2(u)\right], \tag{3.47}$$

where $M = m\upsilon\rho$ is the electron orbital momentum, and $K_v(x)$ are the Mcdonald functions.

Let us analyze in more detail the high-frequency case (3.46), (3.47). First, it is obvious that the spectral distribution described by the variable u does not depend on the initial electron energy E. This suppression of the energy integral is due to the aforementioned electron acceleration in an attractive potential $U(r) = -Ze^2/r$. As a matter of fact, the radiation of large frequencies $\omega \gg \tilde{\omega} = \upsilon/a$ originates from the part of sharp curvature of the impact electron trajectory where its acceleration is maximum. It is obvious that the largest acceleration is observed near the trajectory turning point r_0 (3.43), (3.44). In this domain, the potential energy $U(r_0)$ is much

larger compared with the initial energy ($|U(r_0)| \gg E$) and that is the reason why the latter does not influence the spectral distribution of the emitted energy. This domain for the Coulomb field was first indicated by Kramers (1923). The non-Coulomb generalization of the approximation to suppress the energy integral forms the basis of the so-called Kramers electrodynamics introduced by Kogan et al. (1992).

According to (3.36), the energy spectral distribution consists of the two polarizations corresponding to the rotation directions along and against the electron trajectory. In accordance with the total intensity (3.46, 3.47), the sum of two contributions from two polarizations mentioned is

$$\begin{aligned}\frac{\mathrm{d}E(\rho,\omega)}{\Delta E(\rho)} &= \frac{6}{\pi^2}u^2\left\{\left[K_{1/3}(u)+K_{2/3}(u)\right]^2+\left[K_{1/3}(u)-K_{2/3}(u)\right]^2\right\}\mathrm{d}u \\ &\propto \left[F_-^2(u)+F_+^2(u)\right].\end{aligned} \tag{3.48}$$

It is easy to see that in almost all domains, the change of the function $F_-(u)$ (corresponding to the sum of functions $K_{1/3}$ and $K_{2/3}$) substantially exceeds the function $F_+(u)$ (corresponding to their difference). This particular circumstance is caused mathematically by the compensation of the functions $K_{1/3}$ and $K_{2/3}$ and reflects an important feature of radiation formation in the high-frequency domain; namely, the radiation is basically caused by the electron rotation near the turning point r_0 of the trajectory. The angular velocity of such a rotation $\omega_\mathrm{R}(r_0)$ is defined by the relation:

$$\omega_\mathrm{R}(r_0) = M/mr_0^2 = \sqrt{2(E+|U(r_0)|)/mr_0^2} = \frac{\upsilon_\mathrm{max}}{r_0}, \tag{3.49}$$

where υ_max is the maximum electron velocity.

The aforementioned nature of the spectral formation becomes apparent if one writes down the functions $F_\pm(\omega,E,M)$ for an arbitrary potential $U(r)$ in the form of the Fourier components of the electron trajectory (Kogan and Kukushkin 1984; Kogan et al. 1992):

$$F_\pm(\omega,E,M) = \int\limits_{r_0(E,M)}^{\infty} \frac{\cos\left(\int\limits_{r_0(E,M)}^{\infty}[\omega\pm\omega_\mathrm{R}(r')]\left\{\frac{2}{m}\left[E+|U(r)|-\frac{M\omega_\mathrm{R}(r')}{2}\right]\right\}^{-1/2}\mathrm{d}r'\right)}{\sqrt{E+|U(r)|-\frac{M\omega_\mathrm{R}(r)}{2}}} r\mathrm{d}r. \tag{3.50}$$

For large frequencies $\omega \gg \tilde{\omega}$ the integrated expressions in (3.50) promptly oscillate everywhere, excluding the points of oscillation compensation $\omega \approx \omega_\mathrm{R}(r_\omega)$. The compensation takes place only for the function F_- (which explains the definition of its index) but not for the function F_+. Therefore, the more differ the F_- and F_+ contributions to the intensity $I(\omega)$, the higher the frequency ω becomes. This

circumstance follows from pure classical mechanics and also manifests itself in quantum calculations of transitions probabilities, known as the Bethe rule.

The above analysis of the radiation mechanism in the high-frequency domain reveals a means for an universal spectra description (Kogan et al. 1992). The description is reached by the replacement of the real electron motion by its rotation along a circle with angular velocity $\omega_{\mathrm{R}}(r)$. This approximation is obtained by the introduction of the delta function $\delta[\omega - \omega_{\mathrm{R}}(r)]$ into (3.43), leading to the following spectral distribution (Kogan and Kukushkin 1984; Gervids and Kogan 1991):

$$\left(\frac{\mathrm{d}k}{\mathrm{d}\omega}\right)_{\mathrm{R}} \simeq \frac{8\pi e^2}{3c^3m^2v}\int_0^\infty \left(\frac{\partial U}{\partial r}\right)^2 \sqrt{1-\frac{U(r)}{E}}\, r^2\delta[\omega-\omega_{\mathrm{R}}(r)]\mathrm{d}r. \tag{3.51}$$

Calculation of the integral in (3.51) leads to the following expression for the Gaunt factor (3.40) of the bremsstrahlung (Kogan and Kukushkin 1984; Kogan et al.1992; Gervids and Kogan 1991)

$$g_{\mathrm{rot}}(\omega) = \frac{6}{Z^2e^4}\frac{D_\omega^2}{2+D_\omega}\frac{[E+|U(r_\omega)|]^3}{m\omega^2}, \tag{3.52a}$$

$$D_\omega = -d\ln[E+|U(r_\omega)|]/d\ln r_\omega. \tag{3.52b}$$

In correspondence with the ideas presented above, the radiation radius r_ω is defined by the relation

$$\omega_{\mathrm{R}}(r_\omega) = \omega \tag{3.53a}$$

or

$$\frac{E+|U(r_\omega)|}{r_\omega^2} = \frac{m\omega^2}{2}. \tag{3.53b}$$

The rotational approximation (3.52), (3.53) is of high precision. For example, for a Coulomb potential the error of the approximation does not exceed 5% even for a frequency as low as $\omega = \tilde{\omega}/2$. The detailed analysis of the rotational approximation results in a more general class of atomic potentials (Kogan and Kukushkin 1984; Kogan et al. 1992; Gervids and Kogan 1991).

The supression of the energy integral in the Kramers electrodynamics and the peculiarities of the radiation spectra connected with it work well in the high-frequency domain $\omega \gg \tilde{\omega}$. This domain makes the main contribution to the total bremsstrahlung intensity. As far as the low-frequency domain $\omega \ll \tilde{\omega}$ is concerned, (3.45) shows that there is no compensation of K_0 and K_1 and consequently there is no domination of the spectral function F_- with respect to F_+.

The independence of the radiation characteristics on the energy indicates the universal nature of the radiation spectral dependence on the frequency, not only for

the infinite motion ($E > 0$) considered above but also for the finite motion ($E < 0$) of the electron along an elliptical trajectory, as well. This is easy to verify by analyzing the finite motion intensity distribution $I_n(\omega)$, being the sum of harmonics $n = \omega/\omega_0$, where

$$\omega_0 = (2|E|)^{3/2}/Ze^2\sqrt{m} \tag{3.54}$$

is the typical frequency of the finite motion (the analog of the frequency $\tilde{\omega}$ in a continuum spectrum). The intensity I_n of a given harmonic is equal to (Gervids and Kogan 1991):

$$\begin{aligned} I_n \propto n^2E^4\left(1-\tilde{\varepsilon}^2\right)^2 \\ \times\left\{K_{1/3}^2\left[\frac{n}{3}(1-\tilde{\varepsilon}^2)^{3/2}\right]+K_{2/3}^2\left[\frac{n}{3}\left(1-\tilde{\varepsilon}^2\right)^{3/2}\right]\right\}, \end{aligned} \tag{3.55}$$

where $\tilde{\varepsilon} = (1-2|E|M^2/Z^2me^4)^{1/2}$ is the eccentricity of elliptical trajectory. It is simple to ensure that the argument of the K-functions in (3.55) is reduced, as in the continuum spectrum case, to the universal variable $u \sim M^3\omega/Z^2$. Independence of the spectrum on the energy is realized for the radiation intensity of the classical motion averaged over the period $T = 2\pi/\omega_0$, namely for the quantity (Gervids and Kogan 1991):

$$T\mathrm{d}I = TI_n\mathrm{d}n = \frac{2\pi}{\omega_0}I_n\frac{\mathrm{d}\omega}{\omega_0} \propto \frac{I_n}{\omega_0^2}\mathrm{d}\omega. \tag{3.56}$$

One can see that the quantity (3.56) becomes independent of the electron energy after substitution of (3.55). To summarize, it should be noted that Kramers high-frequency spectral domain possesses a universal intensity distribution for transitions in both continuum and discrete spectra. The universality is connected with the supression of the energy integral for attractive atomic potentials.

3.3.2 *Discrete Energy Spectrum*

Let us consider the results of Kramers electrodynamics (KrED) in the application to transitions in the discrete energy spectrum. As it follows from the general properties of the KrED, the dependencies of spectral characteristics of the radiation remain the same as in the case of a continuous energy spectrum. The only additional fact to be taken into account is the discrete nature of the energy spectrum which corresponds to the following relation between the emitted photon frequency ω and the difference between the initial E_{nl} and final $E_{n'l'}$ atomic state energies:

$$\omega = (E_{\mathrm{nl}} - E_{\mathrm{n}'l'})/\hbar. \tag{3.57}$$

The values for the energies E_{nl} should be taken from the results of quantum mechanical calculations or from corresponding experimental data.

Equation (3.57) leads to the relationship between the spectral interval $\mathrm{d}\omega$ of the emitted photon frequencies and the density $\mathrm{d}n'$ of final states:

$$\mathrm{d}\omega/\mathrm{d}n' = 2\pi/T_{\mathrm{n}'l'}. \tag{3.58}$$

Here, $T_{\mathrm{n}'l'}$ is the period of classical motion (in the general case being only the radial period) of the electron with the energy equal to the energy $E_{\mathrm{n}'l'}$ of the final state. The value T_{nl} is determined by the conventional formulae of classical mechanics (Landau and Lifschitz 2005; Naccache 1972; Kogan and Kukushkin 1984; Kogan et al. 1992) for the case of the central potential $U(r)$.

The general expression for the probability of the transition $\Gamma \to \Gamma'$ ($\Gamma \equiv \{nl\}$) may be obtained from the classical spectral distribution for the emitted energy whose terms are to be separated with respect to the increase and decrease of the electron angular momentum:

$$\Delta E_{\omega}(\rho)_{\pm} = \frac{2e^2 m\omega^4}{3\pi c^3}[F_{\pm}]^2, \tag{3.59}$$

where the functions $F_{\pm}$ defined by (3.50) correspond to the radiation emission processes with the increase (F_{+}) and decrease (F_{-}) of the electron angular momentum.

In order to obtain the probability $W(\Gamma \to \Gamma')$ of a radiative transition per unit time, we divide the quantity (3.59) by the energy $\hbar\omega$ of an emitted photon and by the period T_{nl} of the classical motion with given initial energy and then multiply the result by the final state density (3.58). Thus, we obtain

$$W_{\Gamma\to\Gamma'} = \frac{\Delta E_{\omega}(\rho)}{\hbar\omega}\left|\frac{\mathrm{d}\omega}{\mathrm{d}n'}\right|\frac{1}{T_{\mathrm{nl}}} = \frac{2\pi}{T_{\mathrm{nl}}T_{\mathrm{n}'l'}}\frac{\Delta E_{\omega}(\rho)}{\hbar\omega}. \tag{3.60}$$

Equation (3.60), with account of (3.59) and relation $M = \hbar(l + 1/2) = m\upsilon\rho$, takes the form

$$W(nl \to n'l \pm 1) = \frac{4}{3}\left(\frac{\omega}{c}\right)^3 \frac{me^2}{\hbar}\frac{1}{T_{\mathrm{nl}}T_{\mathrm{n}'l'}}F_{\pm}^2(\omega, l). \tag{3.61}$$

This result coincides with the result of the corresponding quasi-classical calculation (Gantsev et al. 1985; Kogan et al. 1992), in the limit of $n \gg 1$, $l \gg 1$. The periods T_{nl} and $T_{\mathrm{n}'l'}$ in the latter calculation originate from the normalization constants of quasi-classical wave functions (for the relations between the functions $F_{\pm}$ and quasi-classical matrix elements, see Goreslavski et al. (1982), Gantsev et al. (1985), Landau and Lifschitz (1977), Naccache (1972), Kogan and Kukushkin (1984), Kogan et al. (1992)).

The KrED result for a bound–bound transition corresponds to the high-frequency domain where the emitted frequency ω largely exceeds the frequency of the electron revolution around the field center on its classical trajectory:

$$\omega_{nn'} T_{nl} \gg 1. \tag{3.62}$$

The KrED method for the description of an electron bound–bound radiative transition in a central potential $U(r)$ may be considered as some alternative to the well-known quantum defect method (Bates and Damgaard 1949; Davydkin and Zon 1981; Sobelman 1972, 2006; Cowan 1981). The latter is based on the following relation for the final state density

$$\partial\omega/\partial n' = Z_i^2 (\nu_{n'l'})^{-3}, \quad \nu_{n'l'} = n' - \mu_{l'}, \tag{3.63}$$

where $\mu_{1'}$ is the quantum defect value. Equation (3.63) originates from the corresponding dependence in the Coulomb potential generalized onto the case of non-integer quantum number ν_{nl}. The essential feature of the quantum defect method is the use of the Coulomb results for the spectral distribution of the transition probabilities with the subsequent replacement of the originally integer quantum number n by the non-integral quantity ν_{nl}. This approach may be ultimately interpreted as a Coulomb-type approximation for the potential $U(r)$.

It should be noted that the KrED approach does not require such an approximation for the potential. Thus, for free–free radiative transitions (bremsstrahlung) in the field of a many-electron atom, the use of the Thomas–Fermi (TF) potential in (3.39) leads to a successful description of the radiation spectral distribution. The validity of the TF model for the description of bound–bound transitions and the comparison of corresponding results of the KrED with the quantum defect method (Bates and Damgaard 1949) [and its classical analog (Davydkin and Zon 1981)] for the case of an arbitrary deviation of the potential from the Coulomb-type are to be investigated in future.

The most detailed comparison of quasi-classical results for bound–bound transitions with the corresponding quantum numerical calculations has been carried out for the case of the Coulomb field (Gantsev et al. 1985):

$$\sum_{i'=l\pm1} W(nl \to n'l') = 2(l+1/2) G_0\left[\omega(l+1/2)^3/3Z^2\right]/3\pi^2 c^3 (nn')^3, \tag{3.64}$$

where

$$\begin{aligned} G_0(x) &\equiv x\left[K_{1/3}^2(x) + K_{2/3}^2(x)\right] \\ &= \frac{x}{2}\left\{\left[K_{1/3}(x) + K_{2/3}(x)\right]^2 + \left[K_{1/3}(x) - K_{2/3}(x)\right]\right\}^2 \propto x\left[F_-^2(x) + F_+^2(x)\right]. \end{aligned} \tag{3.65}$$

The integration of the spectral probability (3.65) over frequencies gives the total probability (per unit time) of the radiative decay of the state $\{nl\}$:

$$W^{\mathrm{tot}}(nl) = 4Z^4/\pi\sqrt{3}c^3n^3l^2. \tag{3.66}$$

The quantity inverse to (3.66) determines the mean lifetime of this state. Equation (3.66) weighted by the factor $(2l+1)$ and averaged over the values of angular momentum l gives the probability

$$W(n) = \frac{8Z^4\ln(n)}{\pi\sqrt{3}c^3n^5} \tag{3.67}$$

which is close to the results of quantum numerical calculations (Goreslavsky et al. 1982; Gantsev et al. 1985; Bethe and Salpeter 1977) that give (for $n > 20$): $W(n) \approx 7.89 \times 10^9 \cdot \dfrac{Z^4}{n^5} \cdot \left\{3\ln(n) - 0.247\ [\mathrm{s}^{-1}]\right\} \cdot$

Using explicit expressions for the functions F_- and F_+ in the case of the Coulomb potential, it appears possible to trace the origin of the success of the KrED approach. These functions determine the probabilities of transitions with the decrease and increase of the electron angular momentum, respectively. This fact can be proven in the framework of classical radiation theory by calculating the rate of angular momentum loss $\mathrm{d}M/\mathrm{d}\omega\mathrm{d}t$ caused by the classical emission of radiation with frequency ω [e.g., (Landau and Lifschitz 2003; Jackson 2007)]. Though the net rate of the angular momentum change is negative, as it should be, the term containing the function F_+ is positive and therefore corresponds to the increase of the electron angular momentum. Note that the relation between the functions F_+ and F_- indicated is especially transparent within the framework of the quasi-classical approach. In this case, these functions correspond to the transitions with a positive and negative change of the electron orbital quantum number $(\Delta l = \pm 1)$, respectively (3.64), (3.65).

In the Coulomb case, the values of the function $F_-^2(x)$ largely exceed the values of the function $F_+^2(x)$ in a wide range, $x \geq 10^{-2}$. The predominance of the transition with $\Delta l = -1$ over a transition with $\Delta l = +1$ and the growth of this predominance with the growth of the transition frequency $(x \propto \omega M^3)$ constitutes the essence of the well-known Bethe empirical rule (Bethe and Salpeter 1977) derived originally from the results of quantum numerical calculations in the Coulomb case. However, it follows from our consideration (Kogan et al. 1992) that the physical nature of this rule is purely classical. Indeed, this phenomenon can entirely be interpreted classically in terms of the correlation between the angular momentum and polarization of classical radiation. The qualitative explanation can be based on the fact that the intensity of the emission of the radiation, circularly polarized along the direction of the radiating electron rotation, largely exceeds the intensity corresponding to the case of opposite directions of the electron and radiated electric field rotation (the situation is similar, e.g., to the cyclotron radiation emission). The

degree of predominance discussed evidently predetermines the accuracy of the "rotational approximation" (RA). For a Coulomb field, a quantitative estimate of the accuracy of the RA can be found from a comparison of the corresponding contributions of the $\Delta l = \pm 1$ transitions. Their ratio is equal to (Gantsev et al. 1985):

$$\int_0^\infty xF_-^2(x)\mathrm{d}x \Big/ \int_0^\infty xF_+^2(x)\mathrm{d}x = \frac{1+\pi\sqrt{3}/6}{1-\pi\sqrt{3}/6} \approx 20.5\ . \tag{3.68}$$

Thus, the accuray (integral in ω) of the RA is of the order of 5% that agrees with the results of the classical calculations. A detailed numerical comparison of the results of the quantum and quasi-classical calculations for the transition probabilities has been carried out (Gantsev et al. 1985). The result of this calculations of the quantum corrections to the classical limit of the transition probabilities in the Kramers domain is presented in Kogan and Kukushkin (1984).

The degree of deviation of the transition probability from the Bethe rule can be clearly characterized by the function

$$D(x) \equiv xF_+^2(x) = x\left[K_{2/3}(x) - K_{1/3}(x)\right]^2. \tag{3.69}$$

It is appropriate to designate this quantity as the *Bethe rule defect*. A useful analytic approximation of this function is presented in Kogan et al. (1992). The aforementioned predominance of $F_-(x)$ over $F_+(x)$ can be written according to (3.69) in the form of the ratio $D(x)/G_2(x)$ (for G_2 see (3.74) below), which is small in the domain of the applicability of the Bethe rule.

Thus, the KrED method provides the clues for an universal description of the transitions between those discrete spectral energy states which dominantly contribute to the total integral of radiation emission rates. Even for the Coulomb case, in spite of its detailed investigation in the literature (Landau and Lifschitz 1977; Bethe and Salpeter 1977), the KrED approach yields simple analytic results. Thus, the replacement of the Gordon formulae (Bethe and Salpeter 1977) for the transition probabilities by the corresponding KrED formulae appreciably reduces the number of variables since these classical formulae contain a smaller number of independent variables. An application of the KrED method to the non-Coulomb case and a comparison with already existing methods (e.g., the quantum defect method) are subjects for research.

3.4 Radiative Recombination

3.4.1 Kramers Photorecombination Cross Section

The suppression of the energy integral that is fundamental for the KrED approach manifests itself most strongly in the process of photorecombination radiation emission. Indeed, this process is strongly inelastic since the energy $\hbar\omega$ of an emitted photon is in any case larger than the initial energy E of the recombining electron:

$$\hbar\omega = E + |E_{\mathrm{nl}}|, \tag{3.70}$$

where E_{nl} is the energy of electron bound (final) state.

The possibility to suppress the energy integral (see Sect. 3.3) permits the use of the classical approach even for the description of such strongly inelastic process. We shall use the universal classical formula (3.59) for the spectral distribution of the emitted energy to describe the photorecombination cross section. It may be achieved by means of the continuation of the corresponding results for the bremsstrahlung radiation (BR) cross section onto the domain of negative values of the final electron energy with account of its quantization law (3.58).

For the PhR, in contrast to the BR, not only the cross section of the integral over the orbital momentum l is of essential interest, but the cross section $\sigma_{\mathrm{PhR}}(E \to n'l')$, differential with respect to l, as well. In order to obtain $\sigma_{\mathrm{PhR}}(E \to n'l')$, one has to replace the integration over the impact parameters ρ in the BR formulae by a summation over the final state orbital momentum $l' = l \pm 1$:

$$\sigma_{\mathrm{PhR}}\left(E \to n'l'\right) = \frac{\hbar^2 \pi l'}{mE} \frac{\Delta E_{\omega}(l')}{\hbar\omega} \frac{2\pi}{T_{\mathrm{n'l'}}}, \tag{3.71}$$

where the relation $\hbar(l' + 1/2) = \rho m v$ is to be used in $\Delta E_{\omega}(\rho)$. The cross section (3.71) is a functional of the atomic potential $U(r)$ which enters to the spectral functions $F_{-}(\omega)$ and $F_{+}(\omega)$ and for the period $T_{\mathrm{n'l'}}$. A detailed comparison of the quasi-classical result (3.71) with exact quantum computations for the non-Coulomb potentials has not yet been performed. The Coulomb potential (3.71) has been investigated by Kukushkin and Lisitsa (1985), Kim and Pratt (1983). In this case, the spectral dependence of the PhR cross section is described in terms of the universal spectral function $G_0(x)$ (3.65):

$$\sigma_{\mathrm{PhR}}(E \to nl) = 8Z^2(l + 1/2)^2 G_0\left[\omega(l + 1/2)^3/3Z^2\right]/3c^3n^3E. \tag{3.72}$$

Note that (3.72) shows a universal dependence of the cross section on the classical parameter in the argument of the function G_0 similar to the case of the BR.

The total (integral over ρ or l) PhR cross section $\sigma_{\mathrm{PhR}}(E \to n)$ obtained by integration of (3.72) for the Coulomb case is given by

$$\sigma_{\mathrm{PhR}}(E \to n) = \frac{8\pi}{3\sqrt{3}} \frac{Z^4}{c^3 n^3} \frac{1}{E\omega}, \tag{3.73}$$

where $\omega = E + Z^2/2n^2$ (in atomic units). Equation (3.73) is known as Kramers formula.

3.4.2 Radiative Recombination Rates

The analytic result (3.72) allows a derivation of a simple formula for the photorecombination rate q_{nl} into the state with given quantum numbers n and l for a Maxwellian energy distribution with temperature T. Multiplying (3.72) by the electron velocity and then averaging over the Maxwellian velocity distribution, we obtain (Kukushkin and Lisitsa 1985) (in atomic units):

$$q_{\mathrm{PhR}}^{\mathrm{nl}} = 4\left[\frac{2}{2+x_{\mathrm{T}}} G_2(x_{\mathrm{m}}) + \frac{x_{\mathrm{T}}}{2+x_{\mathrm{T}}} \Psi(x_{\mathrm{m}}, x_{\mathrm{T}}) e^{x_{\mathrm{m}} x_{\mathrm{T}}}\right] / \pi^2 n^3 c^3 l^2. \tag{3.74a}$$

Here, the universal dimensionless parameters are introduced:

$$x_{\mathrm{m}} = E_{\mathrm{n}} M^3/3 = (l+1/2)^3/6n^2, \quad x_{\mathrm{T}} = 3/TM^3, \tag{3.74b}$$

which determine the dependencies of the rate q on the level with energy $E = 1/2n^2$ and angular momentum $M = \hbar(l+1/2)$. The function G_2 is related to the universal function G_0 by the equation

$$G_2 = \int_{\mathrm{x}}^{\infty} G_0(x')\mathrm{d}x' = xK_{1/3}(x)K_{2/3}(x) \tag{3.74c}$$

and the function Ψ is expressed in terms of the above-defined "Bethe rule defect" $D(x)$ (3.69):

$$\Psi(x_{\mathrm{m}}, x_{\mathrm{T}}) = \int_{x_{\mathrm{m}}}^{\infty} D(y) \exp(-x_{\mathrm{T}} y)\mathrm{d}y. \tag{3.74d}$$

It follows from (3.74d) that the photorecombination rate is determined by two different terms. In the first term described by the G_2 function, the Bethe rule defect is neglected, whereas the second term is caused exclusively by the Bethe rule defect and becomes appreciable for small x_{m} and large x_{T}.

Thus in the KrED, the PhR rate into the energy state with given n and l quantum numbers is described by an universal function of two parameters. This universal

dependence of the PhR rate in the Kramers domain is in agreement with the exact quantum numerical calculations (as discussed below).

The accuracy of the quasi-classical calculations of the PhR rate turns out to be fairly good (within $\sim 20\%$, according to the results obtained from exact numerical calculations). Detailed tables for the PhR rate in the Coulomb case, obtained in quasi-classical approximation, are presented in Gantsev et al. (1985).

The applicability of KrED analytical results for the Coulomb field case to the description of PhR cross sections for an ion with a core was investigated in detail (Kim and Pratt 1983). The authors use the approximation for the potential of such an ion in the form of a modified Coulomb potential with an effective charge Z_{eff}. It has been shown (Kim and Pratt 1983) that in a wide range of electron energies and ion charges, this Coulomb-type approximation of the potential yields a satisfactory description of the PhR cross sections provided the value Z_{eff} is taken equal to the mean value of the charges of the nuclei Z and of the ion Z_{i}, $Z_{\text{eff}} = (Z + Z_{\text{i}})/2$.

The cross section for the recombination as a function of the Kramers parameter $\omega l^3/Z_{\text{eff}}^2$ for ions with various values of atomic number Z, ion charge Z_{i} and electron energy $E(keV)$ and different sets of parameters Z, Z_{i}, E prove to be satisfactorily described by an universal classical formula with the aforementioned value of Z_{eff}. The same agreement between classical and quantum results occurs also for the dependencies of the cross section on $n(\propto n^{-3})$ which follows from (3.73). The substitution of the Z_{eff} value in this equation gives the following simple analytic approximation for the PhR cross section summed over l (Kim and Pratt 1983):

$$\sigma_{\text{PhR}}^{\text{eff}}(n) = \frac{8\pi}{3\sqrt{3}} Z_{\text{eff}}^4/c^3 n^3 E\left(E + Z_{\text{eff}}^2/2n^2\right). \tag{3.75}$$

The total PhR cross section is obtained by the summation of (3.75) over all allowed (non-occupied) quantum states according to the following equation:

$$\sigma_{\text{PhR}}^{\text{eff}} = W_{\text{n}_0}\sigma_{\text{n}_0} + \sum_{n \geq n_0 + 1} \sigma_{\text{n}}. \tag{3.76}$$

Here, n_0 is the value of the principal quantum number of the filled atomic shell, and W_{n_0} is the statistical weight determined by the ratio of the number of free places in this shell to their total number. The results for the total PhR cross section (3.76) are in good agreement with the results of quantum numerical calculations.

The agreement between the quasi-classical and quantum results may be improved by means of a proper choice of the lower limit of summation $n_{0\text{eff}}$ in (3.76) which depends on the effects of screening and correlations of the electrons in the filled atomic shell. In this case, the value $n_{0\text{eff}}$ will be an universal parameter for a given isoelectronic sequence. Modifying the Kramers formula (3.75), it is easy to obtain an analytical approximation for the total PhR cross section by replacing the summation over n by an integration Kim and Pratt (1983):

$$\sigma^{\mathrm{tot}} \approx \int_{n_{0\mathrm{eff}}}^{\infty} \sigma_{\mathrm{n}} \mathrm{d}n = \frac{8\pi Z_{\mathrm{eff}}^2}{3\sqrt{3}c^3 E} \ln\left(1 + Z_{\mathrm{eff}}^2 / 2En_{0\mathrm{eff}}^2\right). \tag{3.77}$$

The values of the cutoff parameter $s = 1/2n_{0\mathrm{eff}}^2$, obtained from the comparison of (3.77) with the results of quantum calculations, are as follows: $s = 1.1$ for fully stripped ions (bare nuclei), $s = 0.065$ for *Ne*-like shells, $s = 0.045$ for *Ar*-like shells. The numerical quantum results are described satisfactorily by a linear dependence of the logarithm argument on s, namely $(1 + sZ_{\mathrm{eff}}^2/E)$ for $Z_{\mathrm{eff}} = (Z + Z_{\mathrm{i}})/2$.

The simple approximations (3.75), (3.77) for the partial and total PhR cross sections lead to a simple and reliable analytical result (Kim and Pratt 1983) for some important characteristics of a plasma. The rate of photorecombination $\alpha = < \langle \upsilon \sigma^{\mathrm{tot}} \rangle >$ is given by

$$\alpha = \frac{16}{3}\sqrt{\frac{2\pi}{3}} \frac{Z^2 c^{-3}}{\sqrt{T}} [\exp(b) E_1(b) + C + \ln(b)], \quad b = \frac{sZ^2}{T}. \tag{3.78}$$

3.4.3 Radiative Losses

The rate of electron energy loss $\beta = \langle E \upsilon \sigma^{\mathrm{tot}} \rangle$ can be approximated by

$$\beta = \frac{T}{c^2}\left[1 - \frac{16}{3}\sqrt{\frac{2\pi}{3}} \frac{Z^4}{cT^{3/2}} \exp(b) E_1(b)\right]. \tag{3.79}$$

The total rate of radiation losses of plasma due to photorecombination $\gamma = \sum_{\mathrm{n}} \gamma_{\mathrm{n}} = \sum \langle \omega_{\mathrm{n}} \upsilon \sigma_{\mathrm{n}}^{\mathrm{tot}} \rangle$ requires a computation of the sum over n with the aid of approximations for partial cross sections:

$$\gamma = \frac{16}{3}\sqrt{\frac{2\pi}{3}} s \frac{Z^4}{c^3 T^{1/2}}. \tag{3.80}$$

The brackets denote the averaging over the Maxwellian velocity distribution function, $C = 0.577$ is the Euler constant, $E_1(x)$ is the integral exponential function. Comparison with numerical calculations show (Kim and Pratt 1983) that the precision of (3.78, 3.79, 3.80) are considerably improved is one sets $Z = Z_{\mathrm{eff}}$.

3.4.4 Generalized Scaled Empirical Formulas for Radiative Recombination Rates

Quantum mechanical numerical calculations have been performed for the photoionization cross sections. In order to obtain radiative recombination rates, these photoionization cross sections have been transformed with the help of the Milne relation to radiative recombination cross sections:

$$g_{\mathrm{i}}\sigma_{\mathrm{ij}}^{(\mathrm{phi})}(\omega) = \frac{2m_{\mathrm{e}}c^2E}{\hbar^2\omega^2}\, g_{\mathrm{j}}\sigma_{\mathrm{ji}}^{(\mathrm{RR})}(E), \tag{3.81a}$$

$$\hbar\omega = \hbar\omega_0 + E = E_{\mathrm{i}} + E, \tag{3.81b}$$

where E is the energy of the photoelectron. Note that the energy level i corresponds to charge state Z, whereas the level j belongs to charge state $Z + 1$. The rate coefficients of the spontaneous radiative recombination are then given by:

$$R_{\mathrm{ji}}^{\mathrm{spon}} = n_{\mathrm{e}} \int_0^\infty \mathrm{d}E\sigma_{\mathrm{ji}}^{(\mathrm{RR})}(E)\upsilon(E)F(E), \tag{3.82a}$$

where $F(E)$ is the electron energy distribution function of the continuum electrons, n_{e} is the electron density, and $\upsilon(E)$ is the electron velocity given by

$$\upsilon(E) = \sqrt{\frac{2E}{m_{\mathrm{e}}}}. \tag{3.82b}$$

Numerical results have been scaled with respect to charge Z and temperature parameter β and fitted to the following analytical formula for convenient application (P_1, P_2, and P_3 are fitting parameters) (Rosmej et al. 2022):

$$\left\langle \upsilon \cdot \sigma^{(\mathrm{RR})} \right\rangle = 10^{-8} \cdot Z_{\mathrm{eff}} \cdot Q \cdot P_1 \cdot \sqrt{\beta} \cdot \frac{\beta + P_2}{\beta + P_3} \quad \left[\mathrm{cm}^3\,\mathrm{s}^{-1}\right], \tag{3.83a}$$

$$\beta = \frac{Z_{\mathrm{eff}}^2 \cdot Ry}{kT_{\mathrm{e}}}. \tag{3.83b}$$

Ry = 13.606 eV, kT_{e} is the electron temperature in [eV], Z_{eff} is the effective charge determined by $Z_{\mathrm{eff}} = n(E_{\mathrm{n}}(\mathrm{eV})/Ry)^{1/2}$ where E_{n} is the ionization potential of the state n of the ion before recombination and Q is a factor depending on the quantum numbers of angular momentum for the considered transition:

$$Q\left(n_0 l_0^{m-1} SL \rightarrow n_0 l_0^m S_0 L_0\right) = m \cdot \left|G_{\mathrm{SL}}^{S_0 L_0}\right|^2 \cdot \frac{(2S_0+1)(2L_0+1)}{2\cdot(2l_0+1)(2S+1)(2L+1)}. \quad (3.83c)$$

m is the number of equivalent electrons, $G_{\mathrm{SL}}^{S_0 L_0}$ is the fractional parentage coefficient. For example, for radiative recombination into the $4d$-shell from the bare nuclei, we have $n_0 = 4$, $l_0 = 2$, $S_0 = 0.5$, $L_0 = 2$, $m = 1$, $S = 0$, $L = 0$, $G_{\mathrm{SL}}^{S_0 L_0} = 1$ from which it follows $Q(bare\,nuc \rightarrow 4d\,^2D) = 1$. For the radiative recombination into the He-like ground state $1s\,^2S \rightarrow 1s^2\,^1S$, $n_0 = 1$, $l_0 = 0$, $S_0 = 0$, $L_0 = 0$, $m = 2$, $S = 0.5$, $L = 0$, $G_{\mathrm{SL}}^{S_0 L_0} = 1$, it follows $Q(1s\,^2S \rightarrow 1s^2\,^1S) = 0.5$, and for the radiative recombination into the triplet $n = 2$ P-state, i.e. the transition $1s\,^2S \rightarrow 1s2p\,^3P$, $n_0 = 2$, $l_0 = 1$, $S_0 = 1$, $L_0 = 1$, $m = 1$, $S = 0.5$, $L = 0$, $G_{\mathrm{SL}}^{S_0 L_0} = 1$, it follows $Q(1s\,^2S \rightarrow 1s2p\,^3P) = 0.75$.

Table 3.1 shows the numerical result for hydrogen for all nl-states from n = 1–9 and l = 0–8. The before last line provides the sum of the recombination rates over all states with n = 1–9 and l = 0–8 obtained from detailed numerical quantum calculations, whereas the last line provides the sum of the numerical results for n = 1–9 and l = 0–8 and the Kramers approximation for $n > 9$.

Table 3.1 Numerical calculation of the radiative recombination into hydrogen, Q = 1, Z_{eff} = 1 in (3.83)

nl	P_1	P_2	P_3
1s	4.07×10^{-6}	0.05	0.516
2s	6.03×10^{-7}	0.04	0.530
2p	1.57×10^{-6}	0.04	2.59
3s	2.03×10^{-7}	0.06	0.666
3p	5.94×10^{-7}	0.03	2.56
3d	6.52×10^{-7}	0.01	7.39
4s	9.31×10^{-8}	0.06	0.727
4p	2.86×10^{-7}	0.04	2.79
4d	4.10×10^{-7}	0.01	7.49
4f	3.00×10^{-7}	0.01	17.5
5s	5.10×10^{-8}	0.07	0.822
5p	1.57×10^{-7}	0.03	2.78
5d	2.51×10^{-7}	0.01	7.63
5f	2.64×10^{-7}	0.01	17.6
5g	1.39×10^{-7}	0.00	32.4
6s	3.09×10^{-8}	0.07	0.869
6p	9.66×10^{-8}	0.03	2.89
6d	1.61×10^{-7}	0.01	7.79
6f	1.97×10^{-7}	0.01	17.8

(continued)

Table 3.1 (continued)

nl	P_1	P_2	P_3
6*g*	1.58×10^{-7}	0.00	32.5
6*h*	6.74×10^{-8}	0.00	55.8
7*s*	2.03×10^{-8}	0.08	0.954
7*p*	6.37×10^{-8}	0.03	2.98
7*d*	1.09×10^{-7}	0.01	7.94
7*f*	1.44×10^{-7}	0.01	17.9
7*g*	1.39×10^{-7}	0.00	32.6
7*h*	9.44×10^{-8}	0.00	55.7
7*i*	3.33×10^{-8}	0.00	88.5
8*s*	1.41×10^{-8}	0.08	0.989
8*p*	4.43×10^{-8}	0.03	3.06
8*d*	7.71×10^{-8}	0.01	8.09
8*f*	1.06×10^{-7}	0.01	18.1
8*g*	1.14×10^{-7}	0.00	32.8
8*h*	9.58×10^{-8}	0.00	55.9
8*i*	5.53×10^{-8}	0.00	88.1
8*k*	1.48×10^{-8}	0.00	115
9*s*	1.01×10^{-8}	0.08	1.02
9*p*	3.20×10^{-8}	0.03	3.14
9*d*	5.64×10^{-8}	0.01	8.21
9*f*	8.02×10^{-8}	0.01	18.3
9*g*	9.16×10^{-8}	0.00	32.9
9*h*	8.70×10^{-8}	0.00	56.1
9*i*	6.32×10^{-8}	0.00	87.7
9*k*	3.18×10^{-8}	0.00	131
9*l*	5.85×10^{-9}	0.00	127
Total (1*s*...9 *l*)	1.09×10^{-5}	0.16	1.69
Total (1*s*...∞)	1.28×10^{-5}	0.18	2.14

Fitting parameters approximate the numerical results typically accurate better than 10% in the large temperature range $1/8 < \beta < 64$

Table 3.2 shows the numerical result for H-like molybdenum for all nl-states from n = 1–9 and l = 0–8. The before last line provides the sum of the recombination rates over all states with n = 1–9 and l = 0–8 obtained from detailed quantum mechanical calculations, whereas the last line provides the sum of the numerical results for n = 1–9 and l = 0–8 and the Kramers approximation for $n > 9$.

The numerical data have been scaled with respect to Z and β and finally fitted with three parameters. The fitting parameters of Table 3.2 can be used for all ions with $Z > 1$ due to the scaled representation of numerical results. Let us demonstrate an example for application of (3.83), namely radiative recombination into the 6g-state from fully stripped carbon at kT_e = 15.3 eV: $n_0 = 6$, $l_0 = 4$, $S_0 = 0.5$,

$L_0 = 4$, $m = 1$, $S = 0$, $L = 0$, $G_{SL}^{S_0 L_0} = 1$ from which it follows $Q(bare\ nuc \rightarrow 6g\,^2G) = 1$, $Z = Z_{eff} = 6$, $\beta = 32$ and (from Table 3.2) $P_1 = 1.58 \times 10^{-7}$, $P_2 = 0.00$, $P_3 = 32.5$, from which it follows from (3.83a) $\left\langle \upsilon \cdot \sigma^{(RR)}(6g) \right\rangle = 2.66 \times 10^{-14}\,\mathrm{cm^3\,s^{-1}}$. The exact numerical quantum mechanical result calculated specifically for carbon provides $\left\langle \upsilon \cdot \sigma^{(RR)}(6g) \right\rangle = 2.65 \times 10^{-14}\,\mathrm{cm^3 s^{-1}}$. This example demonstrates the high precision of the fitting formulas (3.83) and the advantageous representation of numerical results in Z- and β-scaled representation.

Let us now consider the application of Table 3.2 to estimate the radiative recombination rates for non-hydrogen-like ions with the help of an effective charge Z_{eff}. One of the most difficult tests is the radiative recombination into the ground state of neutral helium, i.e. the transition $1s\,^2S \rightarrow 1s^2\,^1S$. The ionization potential of the helium ground state is $E_i(1s^2\,^1S) = 24.587\,\mathrm{eV}$ from which it follows an effective charge $Z_{eff} = n_0 \cdot \sqrt{E_i/Ry} = 1 \cdot \sqrt{24.587/13.606} = 1.3443$, $Q = 0.5$ and (from Table 3.2) $P_1 = 4.37 \times 10^{-6}$, $P_2 = 0.06$, $P_3 = 0.574$. Let us consider radiative recombination at kT_e = 0.425 eV from which it follows (3.83b) $\beta = Z_{eff}^2 Ry/kT_e = 57.85$ and from (3.83a) $\left\langle \upsilon \cdot \sigma^{(RR)}(1s^2\,^1S) \right\rangle = 2.21 \times 10^{-13}\,\mathrm{cm^3\,s^{-1}}$. The exact numerical quantum mechanical result calculated specifically for the Helium ground state $\left\langle V \cdot \sigma^{(RR)}(1s^2\,^1S) \right\rangle = 2.53 \times 10^{-13}\,\mathrm{cm^3\,s^{-1}}$.

Let us finish with a consideration of the recombination into the triplet n = 2 S-state of He I, i.e. the transition $1s\,^2S \rightarrow 1s2s\,^3S$: $n_0 = 2$, $l_0 = 0$, $S_0 = 1$, $L_0 = 0$, $m = 1$, $S = 0.5$, $L = 0$, $G_{SL}^{S_0 L_0} = 1$ it follows $Q(1s\,^2S \rightarrow 1s2s\,^3S) = 0.75$, $Z_{eff} = n_0 \cdot \sqrt{E_i/Ry} = 2 \cdot \sqrt{4.7677/13.606} = 1.1839$, $Q = 0.75$ and (from Table 3.2) $P_1 = 6.53 \times 10^{-7}$, $P_2 = 0.06$, $P_3 = 0.642$. Let us consider radiative recombination at kT_e = 3.4 eV from which it follows (3.83b) $\beta = Z_{eff}^2 Ry/kT_e = 4.738$ and from (3.83a) $\left\langle \upsilon \cdot \sigma^{(RR)}(1s^2\,^1S) \right\rangle = 0.951 \times 10^{-14}\,\mathrm{cm^3\,s^{-1}}$. The exact numerical quantum mechanical result calculated specifically for the Helium triplet $1s2s\ ^3S$-state provides $\left\langle \upsilon \cdot \sigma^{(RR)}(1s2s\,^3S) \right\rangle = 1.03 \times 10^{-14}\,\mathrm{cm^3\,s^{-1}}$. These examples demonstrate that the use of the generalized scaled fitting parameters of

Table 3.2 Numerical calculation of the radiative recombination into H-like ions, Q = 1, $Z_{eff} = Z_n$

nl	P_1	P_2	P_3
$1s$	4.37×10^{-6}	0.06	0.574
$2s$	6.53×10^{-7}	0.06	0.642
$2p$	1.63×10^{-6}	0.04	2.65
$3s$	2.13×10^{-7}	0.06	0.704
$3p$	6.19×10^{-7}	0.04	2.74
$3d$	6.61×10^{-7}	0.01	7.44
$4s$	9.69×10^{-8}	0.07	0.798

(continued)

Table 3.2 (continued)

nl	P_1	P_2	P_3
$4p$	2.97×10^{-7}	0.04	2.85
$4d$	4.15×10^{-7}	0.01	7.54
$4f$	3.01×10^{-7}	0.01	17.5
$5s$	5.23×10^{-8}	0.07	0.848
$5p$	1.62×10^{-7}	0.04	2.96
$5d$	2.53×10^{-7}	0.01	7.68
$5f$	2.66×10^{-7}	0.01	17.7
$5g$	1.39×10^{-7}	0.00	32.4
$6s$	3.16×10^{-8}	0.07	0.891
$6p$	9.81×10^{-8}	0.03	2.93
$6d$	1.63×10^{-7}	0.01	7.83
$6f$	1.98×10^{-7}	0.01	17.8
$6g$	1.59×10^{-7}	0.00	32.5
$6h$	6.76×10^{-8}	0.00	55.8
$7s$	2.07×10^{-8}	0.08	0.973
$7p$	6.45×10^{-8}	0.03	3.01
$7d$	1.10×10^{-7}	0.01	7.98
$7f$	1.45×10^{-7}	0.01	18.0
$7g$	1.40×10^{-7}	0.00	32.7
$7h$	9.47×10^{-8}	0.00	55.7
$7i$	3.33×10^{-8}	0.00	88.6
$8s$	1.42×10^{-8}	0.08	1.01
$8p$	4.47×10^{-8}	0.03	3.09
$8d$	7.76×10^{-8}	0.01	8.12
$8f$	1.07×10^{-7}	0.01	18.2
$8g$	1.15×10^{-7}	0.00	32.8
$8h$	9.61×10^{-8}	0.00	56.0
$8i$	5.54×10^{-8}	0.00	88.2
$8k$	1.48×10^{-8}	0.00	115
$9s$	1.02×10^{-8}	0.08	1.03
$9p$	3.23×10^{-8}	0.03	3.16
$9d$	5.67×10^{-8}	0.01	8.25
$9f$	8.05×10^{-8}	0.01	18.3
$9g$	9.19×10^{-8}	0.00	33.0
$9h$	8.72×10^{-8}	0.00	56.1
$9i$	6.33×10^{-8}	0.00	87.7
$9k$	3.18×10^{-8}	0.00	131
$9l$	5.86×10^{-9}	0.00	127
Total ($1s \ldots 9l$)	1.09×10^{-5}	0.16	1.69
Total ($1s \ldots \infty$)	1.28×10^{-5}	0.18	2.14

Fitting parameters can also be used for any non-H-like ion with $Z_{\text{eff}} > 1$ in the large temperature range $1/8 < \beta < 64$ because the numerical results have been scaled not only with respect to Z but at the same time with respect to β too. Typical accuracy of fitted rates is 10%

Table 3.2 provide likewise a good accuracy for non-hydrogen-like ions (if the H-like approximation holds true reasonably well) if the charge Z is replaced by the effective charge Z_{eff}. Note, that detailed radiative recombination rates for H I, He I and He II are presented in Annex A.2 and A.3.

3.4.5 *Enhanced Radiative Recombination in Storage Rings*

Several observations in storage rings have identified enhanced radiative recombination by about a factor of 10 at very low energies (Gao et al. 1995, 1997). The essence of the effect is an anomalous increase of recombination rates when the relative energy of the electron–ion collision becomes of comparable value with the transverse electron beam temperature that is of the order of 0.1 meV. The first observations have been made with multicharged ions with a core, and it was suggested that dielectronic recombination might contribute. However, also measurements with bare nuclei indicated enhanced radiative recombination rates by a factor of 4 (Gao et al. 1995). It was found that the excess rates defined as a difference between the measured and standard ones increase sharply as a function of an ion charge (as $Z^{2.8}$) and fall with the increase of the electron energy (Gao et al. 1997). However, for very highly charged ions, the $Z^{2.8}$-scaling could not be confirmed (Hoffknecht et al. 2001).

It has been discussed (Heerlein et al. 2002, 2004a) that three-body recombination can be excluded as an explanation of enhanced rates, as the typical density dependence was not observed. Also Zeeman and Stark effects, stimulated emission, multiphoton effects and QED effects could finally not be made responsible for the enhanced rates, and it was proposed that the observations are driven by an electron distribution function that includes electrons with negative energy when the ions merge the electron beam (Heerlein et al. 2002). However, the modification of the electron distribution function has been controversely discussed (Hörndl et al. 2004; Heerlein et al. 2004b).

In further investigations (Hörndl et al. 2005), dense plasma screening effects as well as B-field effects on the cross sections have been excluded as an explanation for the enhanced rates. In fact, the B-field cross section calculations did not reproduce the observed $B^{0.5}$-field dependence. Finally, transient electric-field-induced enhanced recombination (Hörndl et al. 2005) has been proposed. In this scenario, radiative decay of transiently formed Rydberg states inside the solenoid can stabilize a fraction of these bound electrons by preventing field ionization in the toroidal demerging section. Thus, sufficiently deeply bound electrons with principal quantum numbers contribute, in addition to the RR channel, to the observed electron ion recombination rate. This model is also geometry dependent, but at present, respective observations have not been possible as all experimental setups are very similar and therefore enhanced radiative recombination rates seem to request further investigations.

3.5 Two-Channel Bremsstrahlung in Electron–Atom Collisions

Photon radiation in scattering of a charged particle by an atom (ion, molecule, cluster, etc.) is called *bremsstrahlung*. The initial and final states of a radiating particle in this process belong to the continuous spectrum, and radiation energy originates from its kinetic energy. Let us consider at first a simple case when a nonrelativistic electron is scattered by a "bare" nucleus (that is, a nucleus without bound electrons) with a charge number Z. We use the classical expression for the dipole radiation power Q in terms of acceleration $\boldsymbol{w}$ of a scattered electron (an acceleration of a nucleus can be neglected because of its heavy mass):

$$Q(t) = \frac{2e^2}{3c^3} w^2(t). \tag{3.84}$$

The total energy of the bremsstrahlung is

$$E = \frac{4e^2}{3c^3} \int_0^\infty |\boldsymbol{w}(\omega)|^2 \frac{\mathrm{d}\omega}{2\pi}. \tag{3.85}$$

In derivation of (3.85), the following relation was used:

$$\int_{-\infty}^{\infty} f^2(t)\mathrm{d}t = 2\int_0^\infty |f(\omega)|^2 \frac{\mathrm{d}\omega}{2\pi}, \tag{3.86}$$

where $f(t)$ is a real function of time and $f(\omega)$ is its Fourier component. To calculate the Fourier component of the acceleration $\boldsymbol{w}(\omega)$, it is necessary to concretize the character of motion of the particle. It is well known that in the case of a central force field the momentum of an electron $M = m\upsilon\rho$ (note that $|\boldsymbol{\upsilon}| = \upsilon$) is conserved, where υ is the electron velocity (at an infinite distance from a nucleus) and, ρ is the impact parameter (see Fig. 3.3).

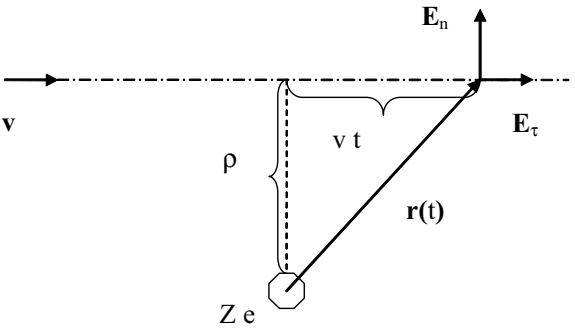

Fig. 3.3 Diagram of electron scattering by a nucleus in the approximation of straight trajectories, ρ is the impact parameter

Thus, the motion of a particle in the potential $U(r = |\boldsymbol{r}|)$ is characterized by two values: the initial velocity and the impact parameter, so the Fourier component of acceleration depends also on ρ: $\boldsymbol{w}(\omega) \to \boldsymbol{w}_\rho(\omega)$. For the last value, we have:

$$\boldsymbol{w}_\rho(\omega) = \frac{e}{m}\boldsymbol{E}(\omega, \rho), \tag{3.87}$$

where $\boldsymbol{E}(\omega, \rho)$ is the Fourier component of the strength of the electric field of a nucleus acting on a scattered electron with a specified impact parameter. Let us calculate $\boldsymbol{E}(\omega, \rho)$ in the *approximation of straight trajectories* of electron motion. This approximation is valid for "distant" collisions, when $\rho > a_C$ ($a_C = Z e^2/m\upsilon^2$ is the Coulomb length). It should be noted that this approach was used by E. Fermi for the calculation of excitation of atoms by charged particles. Using elementary electrodynamic formulas, we find for the Fourier component of the strength of the electric field of a nucleus:

$$\boldsymbol{E}(\omega, \rho) = \frac{2Ze}{\rho\upsilon}\left\{F\left(\frac{\omega\rho}{\upsilon}\right)\boldsymbol{e}_\mathrm{n} - iF'\left(\frac{\omega\rho}{\upsilon}\right)\boldsymbol{e}_\tau\right\}, \tag{3.88}$$

where $\boldsymbol{e}_{\mathrm{n},\tau}$ are the normal and tangent (with respect to the velocity vector $\boldsymbol{\upsilon}$) unit vectors (see Fig. 3.3) and

$$F(\zeta) = \int_0^\infty \frac{\cos(\zeta x)}{(1+x^2)^{3/2}}\mathrm{d}x, \tag{3.89}$$

where the prime ($F'(x)$) denotes differentiation with respect to the argument.

In view of (3.87), it follows from (3.85) an expression for the bremsstrahlung energy differential with respect to photon frequency:

$$\frac{\mathrm{d}E_\rho}{\mathrm{d}\omega} = \frac{2e^4}{3\pi m^2 c^3}|\boldsymbol{E}(\omega, \rho)|^2. \tag{3.90}$$

The probability of bremsstrahlung in a scattering process of an electron with specified impact parameter and frequency is related to the energy of (3.90) by the relation:

$$\frac{\mathrm{d}W_\rho}{\mathrm{d}\omega} = \frac{1}{\hbar\omega}\frac{\mathrm{d}E_\rho}{\mathrm{d}\omega}, \tag{3.91}$$

and the differential (with respect to frequency) cross section is therefore

$$\frac{\mathrm{d}\sigma}{\mathrm{d}\omega} = 2\pi\int_{\rho_\mathrm{min}}^{\rho_\mathrm{max}}\frac{\mathrm{d}W_\rho}{\mathrm{d}\omega}\rho\mathrm{d}\rho. \tag{3.92}$$

$\rho_{\min}$ and $\rho_{\max}$ are the minimum and maximum impact parameters. Gathering the formulas (3.90)–(3.92) together, we obtain:

$$\frac{\mathrm{d}\sigma}{\mathrm{d}\omega} = \frac{4e^4}{3m^2c^3\hbar\omega} \int\limits_{\rho_{\min}}^{\rho_{\max}} |\boldsymbol{E}(\omega,\rho)|^2 \rho \mathrm{d}\rho. \tag{3.93}$$

Hence, in the approximation of straight trajectories, we have obtained for the spectrally resolved cross section for the electron bremsstrahlung in the field of a "bare" nucleus:

$$\frac{\mathrm{d}\sigma}{\mathrm{d}\omega} = \frac{16Z^2e^6}{3m^2\upsilon^2c^3\hbar\omega} \int\limits_{\rho_{\min}}^{\rho_{\max}} \frac{\mathrm{d}\rho}{\rho} \left\{ F^2\left(\frac{\omega\rho}{\upsilon}\right) + F'^2\left(\frac{\omega\rho}{\upsilon}\right) \right\}, \tag{3.94}$$

where the function $F(\zeta)$ is given by the formula (3.89).

Classical consideration is found to be insufficient for the determination of the limits of integration $\rho_{\min}$, $\rho_{\max}$ in (3.94). For this purpose, it is necessary to invoke quantum considerations. For example, the minimum value $\rho_{\min}$ is defined by the de Broglie wavelength of a scattered electron:

$$\rho_{\min} \approx \lambda_{\mathrm{DB}}/2\pi = \frac{\hbar}{m\upsilon}. \tag{3.95}$$

The relation (3.95) reflects the fact that the location of a quantum particle cannot be determined more exactly than spatial "diffusiveness" of its wave function that is characterized by the de Broglie wavelength. To determine the maximum impact parameter $\rho_{\max}$, it is necessary to use the law of conservation of energy and the relation between the change of momentum Δp of an incident electron and the impact parameter ρ: $\Delta p \approx \hbar/\rho$. Then, it can be obtained:

$$\rho_{\max} \approx \frac{\upsilon}{\omega}. \tag{3.96}$$

In derivation of (3.96), the energy conservation law was used in the form $\hbar\omega = \boldsymbol{\upsilon}\,\Delta\boldsymbol{p}$ that is true for small changes of an electron momentum $|\Delta\boldsymbol{p}| \ll p$, which corresponds to the approximation of straight trajectories. This approximation realized in case of distant collisions $\rho > a_{\mathrm{C}}$ implies the weakness of interaction of a projectile with the target (nucleus). Naturally, in weak interaction mainly low-frequency photons will be emitted. It can be shown that a corresponding condition looks like: $\omega < \omega_{\mathrm{C}}$, where $\omega_{\mathrm{C}} = \upsilon/a_{\mathrm{C}}$ is the Coulomb frequency. In the low-frequency region, the argument of the function $F(\zeta)$ and of its derivative $F'(\zeta)$ is less than one: $\zeta = \omega\,\rho/\upsilon < 1$, so, as it follows from the definition (3.89), the following approximate equalities can be used: $F(\zeta) \approx 1$ and $F'(\zeta) \approx 0$. As a result, instead of (3.94) we have:

$$\frac{\mathrm{d}\sigma}{\mathrm{d}\omega} = \frac{16Z^2e^6}{3m^2v^2c^3\hbar\omega}\ln\left(\frac{\rho_{\max}}{\rho_{\min}}\right). \tag{3.97}$$

It is easy to generalize the obtained expression to an arbitrary scattered particle, for which the used approximations are fulfilled. For this purpose, it is necessary to make replacements in the formulas (3.84) and (3.87) according to $e \to e_\mathrm{p}$, $m \to m_\mathrm{p}$, where e_p and m_p are the charge and the mass of the projectile. Then, in view of (3.95) and (3.96) we obtain from (3.97) the expression for the spectral bremsstrahlung of a nonrelativistic charged particle on a "bare" nucleus in the low-frequency approximation ($\hbar\omega \ll m_\mathrm{p}v^2/2$):

$$\frac{\mathrm{d}\sigma}{\mathrm{d}\omega} = \frac{16Z^2e^2e_\mathrm{p}^4}{3m_\mathrm{p}^2v^2c^3\hbar\omega}\ln\left(\frac{m_\mathrm{p}v^2}{\hbar\omega}\right). \tag{3.98}$$

From the obtained equation, it follows that the bremsstrahlung cross section is *inversely proportional to the squared mass of the projectile*. Thus, in going from light charged particles (electron, positron) to heavy particles (proton, alpha particle, etc.), the cross section of the process under consideration decreases more than million times. This conclusion led to the well-known statement that heavy charged particles do not emit bremsstrahlung photons. As it will be clear from the following, this statement needs considerable correction.

The spectral intensity of radiation is equal to the process cross section multiplied by the projectile flux and the energy of an emitted photon, so (3.98) gives:

$$\frac{\mathrm{d}I}{\mathrm{d}\omega} = \frac{16Z^2e^2e_\mathrm{p}^4}{3m_\mathrm{p}^2vc^3}\ln\left(\frac{m_\mathrm{p}v^2}{\hbar\omega}\right). \tag{3.99}$$

As discussed above, the formulas (3.98), (3.99) were obtained in the approximation of distant collisions corresponding to emission of low-frequency photons. The contribution of high-frequency photons $\omega > \omega_\mathrm{C}$ to the bremsstrahlung is made by close collisions $\rho < a_\mathrm{C}$ corresponding to strongly curved trajectories. The spectral cross section and intensity of the electron bremsstrahlung in this case are described by the Kramers formulas:

$$\frac{\mathrm{d}\sigma^{(\mathrm{Kram})}}{\mathrm{d}\omega} = \frac{16\pi Z^2e^6}{3\sqrt{3}m^2v^2c^3\hbar\omega}, \tag{3.100}$$

$$\frac{\mathrm{d}I^{(\mathrm{Kram})}}{\mathrm{d}\omega} = \frac{16\pi Z^2e^6}{3\sqrt{3}m^2vc^3}. \tag{3.101}$$

The right-hand side of the (3.101) does not include the Planck constant, which is indicative of a purely classical nature of this expression.

It is interesting to note that the Kramers formulas describe not only bremsstrahlung, but also photorecombination, when the final state of a radiating electron belongs to the discrete ion spectrum. This circumstance follows from the fact that radiation in the high-frequency limit $\omega > \omega_C$ is "gathered" from a section of the trajectory of closest approach to the nucleus, so a radiating electron "does not know" where it is scattered after emission of a photon.

The expressions (3.98)–(3.99) were obtained within the framework of classical consideration with quantum "insertions" (3.95), (3.96). It is clear that such an approach is not consistent, but its important advantage is physical transparency and mathematical simplicity. It is pertinent to note here that the use of the quantum mechanical formalism within the framework of the *Born approximation* results in the same formulas for the cross section and intensity of bremsstrahlung of low-frequency photons as (3.98), (3.99).

The criterion of the Born approximation is given by the relation:

$$\frac{Z\left|ee_{\mathrm{p}}\right|}{\hbar v} \ll 1, \tag{3.102}$$

Relation (3.102) corresponds to sufficiently fast projectiles. The condition (3.102) allows calculation of the scattering cross section according to the perturbation theory; the ratio $Z\left|ee_{\mathrm{p}}\right|/\hbar v$ serves as a small parameter in the theory. The possibility of classical consideration is given by an inequality that is reverse to (3.102), so the above coincidence of results is to a certain extent by accident. A similar accidental coincidence of classical and quantum results holds true for the Rutherford cross section of electron scattering by a nucleus.

3.6 Bremsstrahlung in Many Electron–Atom Collisions and Mass-Independent Radiation

When going to bremsstrahlung on an atom, it is necessary to take into account the screening effect of bound electrons, resulting in the replacement

$$\rho_{\max} \to \min(v/\omega, r_{\mathrm{a}}), \tag{3.103}$$

(r_{a} is the atomic radius) in the expressions for the cross section and intensity. In fact, for impact parameters $\rho > r_{\mathrm{a}}$ the atomic field is equal to zero, so the acceleration of a projectile vanishes, and, according to (3.84), the bremsstrahlung vanishes too. It is obvious that screening is essential for sufficiently low frequencies $\omega < v/r_{\mathrm{a}}$; otherwise, a projectile should pass sufficiently close to the nucleus to emit a photon at specified frequency.

In case of bremsstrahlung on multielectron atoms, when the Thomas–Fermi model is valid, the Thomas–Fermi radius can be used as an atomic radius:

$r_a \approx r_{TF} = a_B b/\sqrt[3]{Z}$, where $a_B \approx 0.53$ Å is the Bohr radius, Z is the charge number of the atomic nucleus, and $b \cong 0.8553$ is a constant.

The replacement (3.103) corresponds to the *screening approximation* in the bremsstrahlung theory used by H. Bethe and W. Heitler to generalize the cross section formulas to the atomic case. Physically, the screening approximation means the replacement of atomic electrons by a nucleus with effective charge. Thus, bound electrons are excluded from consideration as a dynamical degree of freedom that might occur during bremsstrahlung. In fact, during emission of high-energy photons an energy–momentum excess can be transferred to atomic electrons, resulting in their excitation and ionization.

Besides a real excitation, atomic electrons can be excited *virtually* in a collision of an atom with a charged particle. Virtual excitation corresponds to the occurrence of a variable dipole moment in an atom that, according to the fundamentals of electrodynamics, should radiate electromagnetic waves. Such a process is called *polarization bremsstrahlung* since it is connected with the dynamic polarizability of an atom defining a radiating dipole moment.

Polarization bremsstrahlung can be interpreted also as a process of scattering of the eigenfield of a projectile (a virtual photon) contributing to the radiation field (a real photon) of atomic electrons. Polarization bremsstrahlung is therefore an additional radiation channel in charge scattering by a target with a system of bound electrons. We will call a bremsstrahlung that exists also on a "bare" nucleus ordinary or static bremsstrahlung. The latter term implies that this channel is the only channel in the model of static distribution of the electron charge of bound electrons.

Let us derive formulas for the polarization bremsstrahlung of a fast charged particle on an atom, considering the atom to be an elementary dipole with polarizability $\beta(\omega)$. For the description of the projectile motion, we use, as above, the classical approach and the approximation of straight trajectories. We proceed from the formula for dipole radiation power, but this time we will formulate it in terms of the dipole moment of the radiating system:

$$Q(t) = \frac{2}{3c^3}\left|\ddot{\boldsymbol{d}}(t)\right|^2. \tag{3.104}$$

Here, two dots denote the second time derivative. Integrating the (3.104) with respect to time and using the formula (3.87) for the squared second derivative of the dipole moment, we come to the expression for the total energy of polarization bremsstrahlung for the time of a collision corresponding to the impact parameter ρ:

$$E = \frac{4e^2}{3c^3}\int_0^\infty \omega^4\left|\beta(\omega)\boldsymbol{E}^{(p)}(\omega,\rho)\right|^2\frac{\mathrm{d}\omega}{2\pi}, \tag{3.105}$$

where $\boldsymbol{E}^{(p)}(\omega,\rho)$ is the Fourier component of the strength of the electric field of a charged projectile at the location of an atom. In derivation of this formula, the

relation $\ddot{\boldsymbol{d}}(\omega) = -\omega^2 \boldsymbol{d}(\omega)$ was used that follows from the definition of the Fourier components.

Going from the total radiated energy to the spectral cross section as was done in derivation of the formula (3.93), we obtain the following expression for the polarization bremsstrahlung:

$$\frac{\mathrm{d}\sigma^{\mathrm{PB}}}{\mathrm{d}\omega} = \frac{4\omega^3 |\beta(\omega)|^2}{3c^3\hbar} \int\limits_{\tilde{\rho}_{\min}}^{\tilde{\rho}_{\max}} \left| \boldsymbol{E}^{(p)}(\omega, \rho) \right|^2 \rho \, \mathrm{d}\rho. \tag{3.106}$$

The upper limit of integration in this formula follows from the energy conservation law (3.96), being of the same value as for static bremsstrahlung. But the lower limit of integration is essentially different. In the elementary dipole approximation under consideration, it is defined by the size of an atom:

$$\tilde{\rho}_{\min} = r_{\mathrm{a}}. \tag{3.107}$$

As the analysis shows, scattering with small impact parameters $\rho < r_{\mathrm{a}}$ makes small contributions to the polarization bremsstrahlung cross section since in this case the coherence in re-emission of the projectile eigenfield by atomic electrons to a real photon is lost.

From Fig. 3.3, it is easy to see that the Fourier component of the strength of the electric field of a projectile in the approximation of straight trajectories can be calculated by a formula similar to (3.88), with replacement of the nuclear charge by the projectile charge. As a result, for the strength $\boldsymbol{E}^{(p)}(\omega, \rho)$ we have:

$$\boldsymbol{E}^{(p)}(\omega, \rho) = \frac{2e_{\mathrm{p}}}{\rho\upsilon} \left\{ -F\left(\frac{\omega\rho}{\upsilon}\right) \boldsymbol{e}_{\mathrm{n}} + iF'\left(\frac{\omega\rho}{\upsilon}\right) \boldsymbol{e}_{\tau} \right\}, \tag{3.108}$$

where $\boldsymbol{e}_{\mathrm{n}}$ and $\boldsymbol{e}_{\tau}$ are the normal and tangent unit vectors, and the function $F(\zeta)$ is given by the (3.89). Substituting (3.108) in (3.106), we obtain the spectral cross section of polarization bremsstrahlung:

$$\frac{\mathrm{d}\sigma^{\mathrm{PB}}}{\mathrm{d}\omega} = \frac{16e_{\mathrm{p}}^2\omega^3 |\beta(\omega)|^2}{3\upsilon^2 c^3 \hbar} \int\limits_{r_{\mathrm{a}}}^{\upsilon/\omega} \frac{\mathrm{d}\rho}{\rho} \left\{ F^2\left(\frac{\omega\rho}{\upsilon}\right) + F'^2\left(\frac{\omega\rho}{\upsilon}\right) \right\} \mathrm{d}\rho. \tag{3.109}$$

Hence, we find for the intensity:

$$\frac{\mathrm{d}I^{\mathrm{PB}}}{\mathrm{d}\omega} = \frac{16e_{\mathrm{p}}^2\omega^4 |\beta(\omega)|^2}{3\upsilon c^3} \int\limits_{r_{\mathrm{a}}}^{\upsilon/\omega} \frac{\mathrm{d}\rho}{\rho} \left\{ F^2\left(\frac{\omega\rho}{\upsilon}\right) + F'^2\left(\frac{\omega\rho}{\upsilon}\right) \right\} \mathrm{d}\rho. \tag{3.110}$$

It should be noted that the formula (3.110) does not contain the Planck constant, which is indicative of the classical nature of the polarization bremsstrahlung.

In the low-frequency limit, when $F(\zeta) \approx 1$ and $F'(\zeta) \approx 0$, the formula (3.109) gives:

$$\frac{\mathrm{d}\sigma^{\mathrm{PB}}}{\mathrm{d}\omega} = \frac{16 e_{\mathrm{p}}^2 \omega^3 |\beta(\omega)|^2}{3\upsilon^2 c^3 \hbar} \ln\left(\frac{\upsilon}{\omega r_{\mathrm{a}}}\right). \tag{3.111}$$

This expression is valid for frequencies $\omega < \upsilon/r_{\mathrm{a}}$; otherwise, it is necessary to employ formula (3.109). However, the calculation shows that in the frequency range $\omega > \upsilon/r_{\mathrm{a}}$ polarization bremsstrahlung is low.

The cross section (3.111) can be obtained within the framework of the quantum approach in the domain of validity of the Born approximation (3.92), that means for fast (but nonrelativistic) projectiles.

It should be emphasized that the polarization bremsstrahlung cross sections (3.109), (3.111) do not depend on the projectile mass in contrast to the static bremsstrahlung cross section (3.99). Thus, the long existing statement in physics that heavy charged particles do not emit bremsstrahlung photons does not extend to the polarization channel. This circumstance is connected with the fact that the static bremsstrahlung cross section is proportional to the squared acceleration of a projectile, while the polarization cross section does not depend on this acceleration.

The polarization bremsstrahlung cross section (3.111) can be obtained from the static cross section (3.98) via the replacements $m_{\mathrm{p}} \to m$, $e_{\mathrm{p}}^4 \to e^2 e_{\mathrm{p}}^2$, $\rho_{\min} \to \tilde{\rho}_{\min}$ and

$$Z \to Z_{\mathrm{pol}}(\omega), \tag{3.112}$$

where

$$Z_{\mathrm{pol}}(\omega) = \frac{m\omega^2}{e^2} |\beta(\omega)|^2 \tag{3.113}$$

is the effective polarization atomic charge (in units of the electron charge e) (Rosmej et al. 2017). A polarization charge characterizes the ability of the electron core of an atom to emit a photon under the action of an ac field. In contrast to an ordinary charge, a polarization charge depends on radiation frequency. The frequency dependence of polarization charges of silver and krypton atoms is presented in Fig. 3.4.

From Fig. 3.4, it is seen that in the high-frequency range the polarization charge is equal to the number of bound electrons of an atom (or the charge number of its nucleus). This fact follows from the definition (3.113) and the formula for high-frequency polarizability (2.43). In the low-frequency region $\omega \to 0$ a polarization charge, according to (3.113), decreases quadratically since in this case atomic polarizability is equal to its static value (2.42) that does not depend on frequency. Finally, in the intermediate spectral range the polarization charge is a non-monotonic

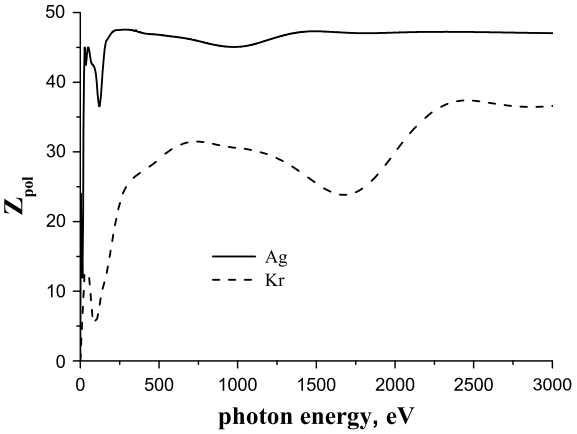

Fig. 3.4 Spectral dependence of the polarization charges of silver and krypton atoms

function that reflects the features of the energy spectrum of an atom. For example, a wide "dip" in the dashed curve of Fig. 3.4 in the range of 1600–1750 eV corresponds to the binding energy for $2p$-electrons in the krypton atom. A minimum in the low-frequency region corresponds to virtual excitation of atomic subshells with principal quantum number $n = 3$. Thus, the spectral cross section of polarization bremsstrahlung reflects the atomic core dynamics as a function of frequency.

In the high-frequency limit, when $\omega \gg \omega_a$(ω_a is the characteristic frequency of excitation of an atom in the discrete spectrum), but still $\omega < \upsilon/r_a$, $\beta(\omega) \approx -Ze^2/m\omega^2$ ($Z_{pol}(\omega) = Z$) the formula (3.111) gives:

$$\frac{d\sigma^{PB}}{d\omega} = \frac{16Z^2e^4e_p^2}{3m^2\upsilon^2c^3\hbar\omega}\ln\left(\frac{\upsilon}{\omega r_a}\right). \tag{3.114}$$

Curiously, in case of an incident electron (positron), the obtained expression differs from the formula for the static bremsstrahlung cross section only by the logarithmic factor.

Let us now consider the resonance case, when the bremsstrahlung frequency is close to one of the eigenfrequencies of an atom, i.e. $\omega \approx \omega_0$. The dynamic polarizability looks like

$$\beta(\omega \approx \omega_0) \cong \frac{e^2}{m}\frac{f_0}{\omega_0^2 - \omega^2 - 2i\omega\gamma_0}. \tag{3.115}$$

This expression for the resonance polarizability follows from the general formula (2.41) if only the resonance summand is considered for which $\omega_{nm} \equiv \omega_0, f_{nm} \equiv f_0$, and $\gamma_{nm} \equiv \gamma_0$. Substituting the formula (3.115) in (3.111), we obtain:

$$\frac{\mathrm{d}\sigma^{\mathrm{res}}}{\mathrm{d}\omega} = \frac{4}{3}\frac{e_{\mathrm{p}}^2}{\hbar c}\left(\frac{c}{\upsilon}\right)^2 \frac{r_{\mathrm{e}}^2 f_0^2 \omega_0}{\left(\omega_0 - \omega\right)^2 + \gamma_0^2} \ln\left(\frac{\upsilon}{\omega r_{\mathrm{a}}}\right), \tag{3.116}$$

where $r_{\mathrm{e}} = e^2/mc^2 \approx 2.8 \times 10^{-13}$ cm is the classical radius of an electron.

From the expression (3.116), it is seen that resonance polarization bremsstrahlung has a sharp maximum at the frequency $\omega = \omega_0$ if $\gamma_0 \ll \omega_0$. The last inequality is satisfied in case of excitation of electrons of the outer atomic shell into the discrete spectrum. For neutral atoms, energies of the resonant photons are about 10 eV. In case of multiply charged ions with a system of bound electrons (an electron core), these energies can be much higher and reach values of the order of several keV. However, in this case the transition damping constant being equal to the Einstein coefficient A_{mn} is also large, and therefore, the resonance is not sharp anymore. At frequencies corresponding to virtual excitation of inner atomic shells, the resonance structure in the spectral dependence of the dynamic polarizability $\beta(\omega)$ disappears. In the spectral curves, "dips" appear that correspond to the beginning of the photoionization of an atomic subshell (see Fig. 3.4).

Thus, resonance effects in the above-considered *spontaneous* polarization bremsstrahlung are essential only in a narrow frequency interval in the vicinity of a resonance and are ill-defined in the integral characteristics of radiation. The situation changes when going to the *induced* bremsstrahlung (also called the *induced bremsstrahlung effect*).

3.7 Photoionization

3.7.1 General Relations

Let us consider at first a bound–free transition of a quantum system with photon absorption under the action of electromagnetic radiation of moderate intensity, when the condition of applicability of the perturbation theory is satisfied. Let the atom be excited as a result of absorption of a photon of an external field. Photoabsorption is characterized by the spectral cross section that is connected with the probability per unit time for excitation of a bound electron under the action of electromagnetic radiation with a specified frequency ω. For the photoabsorption cross section $\sigma(\omega)$, there exist a number of general relations that are used for the construction of approximate models to quantitatively describe the photoeffect. For example, it is convenient to express the value $\sigma(\omega)$ in terms of the *spectral function of dipole excitations* $g(\omega)$ according to the formula (Amusia 1990):

$$\sigma(\omega) = \frac{2\pi^2}{137} a_{\mathrm{B}} \upsilon_{\mathrm{a}} g(\omega), \tag{3.117}$$

where a_B is the Bohr radius, and $\upsilon_a \cong 2.18 \times 10^8$ cm/s is the velocity of an electron in the first Bohr orbit in a hydrogen atom (an atomic unit of velocity). Hereafter, the number 137 resulted from writing the velocity of light in atomic units: $c/\upsilon_a \cong 137$. The function $g(\omega)$ is very convenient because it satisfies the sum rule:

$$\int g(\omega)\mathrm{d}\omega = N_n, \tag{3.118}$$

where N_n is the total number of electrons in an atomic shell n. Besides, the spectral function $g(\omega)$ satisfies also the equation:

$$g(\omega) = \sum_j f_{ij}\delta(\omega - \omega_{ij}), \tag{3.119}$$

where f_{ij} is the strength of an oscillator for the transition $i \to j$ and ω_{ij} is the eigenfrequency of this transition. It should be noted that if we are dealing with the photoionization of an electron in subshell nl with specified principal n and orbital l quantum numbers, the expressions (3.117)–(3.119) should be related to this subshell and designated with corresponding indices: X_{nl}.

The above formulas (3.117)–(3.119) concern not only photoionization, but also photoabsorption that is accompanied by electron transitions in the discrete spectrum, i.e. photoexcitation. In case of a photoionization, the summation in (3.119) is replaced by an integration over states of the continuous spectrum, the integrand being a differential oscillator strength for transition to the continuum $\mathrm{d}f/\mathrm{d}\varepsilon$, where ε is the energy of a state of the continuous spectrum of an electron. The differential oscillator strength is expressed in terms of the matrix element $d_{i\varepsilon}$ of a transition dipole moment operator for transitions to the continuum in the same manner as for transitions to the discrete spectrum:

$$\frac{\mathrm{d}f}{\mathrm{d}\varepsilon} = \frac{2\omega|d_{i\varepsilon}|^2}{3e^2a_B^2}, \tag{3.120}$$

where e is the elementary charge.

It is useful to introduce the concept of an oscillator strength density for transitions into the discrete spectrum too. The oscillator strength of such transitions has to be divided by the energy interval from the given level to the nearest energy level. It can be shown that in this case the following relation is valid (Cowan 1981; Sobelman 1972, 2006):

$$\lim_{n'\to\infty} \frac{4\pi^2 Rya_B^2}{137} \frac{f_{nl,n'l'}}{E_{n'+1l'} - E_{n'l'}} = \sigma_{nl,\varepsilon l'}(I_{nl}). \tag{3.121}$$

This means, the normalized oscillator strength density for infinitely large principal quantum numbers goes over to the threshold value of the partial (corresponding to a given value of orbital quantum number l') cross section of photoionization of an

electron subshell *nl*. The limiting transition (3.121) is a demonstration of a smooth conjugation of optical characteristics of discrete and continuous spectra.

The most general expression for the cross section of photoionization of an electron subshell in the one-electron approximation (that is, with neglect of inter-electron correlations) looks like

$$\sigma_{\mathrm{nl}}(\omega) = \frac{4\pi^2 N_{\mathrm{nl}} \upsilon_a}{3e^2 a_{\mathrm{B}} \omega 137(2l+1)} \left[\left| d_{\mathrm{nl},\varepsilon(l+1)} \right|^2 + \left| d_{\mathrm{nl},\varepsilon(l-1)} \right|^2 \right], \tag{3.122}$$

where N_{nl} is the number of equivalent electrons, that is, electrons with the same values of principal and orbital quantum numbers. Here, there are introduced the matrix elements of a dipole moment operator for transitions to states of the continuous spectrum with orbital quantum numbers allowed by selection rules. These matrix elements can be expressed in terms of radial wave functions of the initial $(R_{\mathrm{nl}}(r))$ and final $(R_{\varepsilon l'})$ states as follows:

$$d^r_{\mathrm{nl},\varepsilon l'} = \frac{e\omega \upsilon_{\mathrm{a}}}{a_{\mathrm{B}}} \sqrt{(2l+1)(2l'+1)} \begin{pmatrix} l & 1 & l' \\ 0 & 0 & 0 \end{pmatrix} \int_0^\infty R_{\mathrm{nl}}(r) r R_{\varepsilon l'}(r) r^2 \mathrm{d}r, \tag{3.123}$$

where $\begin{pmatrix} l & 1 & l' \\ 0 & 0 & 0 \end{pmatrix}$ is the so-called $3j$-symbol. It results from integration with respect to angular variables in the definition of the matrix element of the dipole moment. The $3j$ symbol describes the *selection rules for dipole radiation*, according to which $l' = l \pm 1$. Naturally, in the case $l = 0$ there is one allowed value of a quantum number of an orbital moment in the final state: $l' = 1$. As a rule, the main contribution to the photoionization cross section is made by a transition with increasing quantum number of an orbital moment $l \to l+1$. Exceptions to this rule occur if for some specific reasons the matrix element $d_{\mathrm{nl},\mathrm{n}'l+1}$ is small or goes to zero. On the other hand for the angular distribution of ionized electrons (that we do not consider here), the transition $l \to l-1$ can play an important role.

3.7.2 Hydrogen-like Approximation

As was shown for the first time by Sommerfeld (1978), the total (integrated with respect to the electron escape angle) photoionization cross section for the ground $1s$-state of a hydrogen-like ion is

$$\sigma^{\mathrm{H-like}}_{\mathrm{ph}\ 1s}(\omega) = \frac{2^9 \pi^2}{3Z^2 137} \left(\frac{I_{1\mathrm{s}}}{\hbar\omega} \right)^4 a_{\mathrm{B}}^2 \frac{\exp(-4\zeta arcctg\zeta)}{1 - \exp(-2\pi\zeta)}, \tag{3.124}$$

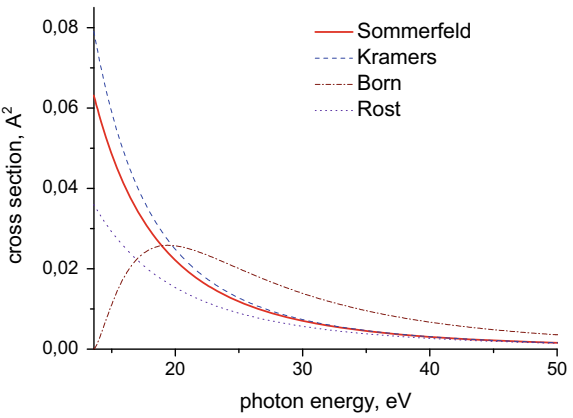

Fig. 3.5 Sommerfeld, Kramers, and Born cross sections of photoionization of the ground state of a hydrogen atom and the cross section in the Rost approximation

where ω is the ionizing radiation frequency, Z is the nuclear charge, $I_{1s} = Z^2 Ry$ is the ionization potential of the $1s$-state (Ry=13.6 eV), $p = \sqrt{2m(\hbar\omega - I_{1s})}$ is the momentum of the ionized electron, and $\zeta = Zme^2/p\hbar$ is the so-called *Born parameter*. The Born parameter (see also (3.102)) is a dimensionless quantity characterizing the force of interaction between an electron and a charged particle. This parameter is introduced in the electron scattering theory and usually written in terms of the electron velocity: $\zeta = Ze^2/\hbar v$. The dependence of the Sommerfeld photoeffect cross section (3.124) on the photon energy is presented in Fig. 3.5 (solid curve).

It should be noted that photoionization is a process of the first order with a smallness parameter being the electromagnetic interaction constant ($e^2/\hbar c \cong 1/137$ in ordinary units). This manifests itself in the presence of the velocity of light (the number 137) to the first power in the denominator of the formula (3.124).

In the vicinity of the photoionization threshold, when $p \to 0, \quad \zeta \to \infty$, we obtain from the formula (3.124) the following approximate expression for the photoeffect cross section:

$$\sigma_{1s}(\omega) \approx \frac{2^9 \pi^2 a_B^2}{3e^4 Z^2 137}\left(1 - \frac{8}{3}\frac{(\hbar\omega - I_{1s})}{I_{1s}}\right) \approx \frac{0.23 a_B^2}{Z^2}\left(1 - \frac{8}{3}\frac{(\hbar\omega - I_{1s})}{I_{1s}}\right), \quad (3.125)$$

where e is the base of the natural logarithm (not to be confused with an elementary charge). Thus, the photoeffect cross section for a hydrogen atom ($Z = 1$) at the threshold ($\hbar\omega = Ry$) is equal to 0.063 Å^2 or 6.3 Mb. It should be noted that the cross section of photoionization of atoms is often given in megabarns: 1 Mb = 10^{-18} cm^2.

An important feature of the photoeffect of hydrogen-like atoms follows from formulas (3.124)–(3.125): The maximum of the cross section value is achieved at threshold, that is, at the minimum radiation frequency, at which photoionization is

still possible. For higher frequencies, the cross section monotonically decreases. This property is caused by the fact that an ionized electron experiences Coulomb attraction of a nucleus that increases the cross section.

From the formula (3.125), it follows that the cross section of photoionization of the ground state of a hydrogen-like ion decreases at the threshold inverse proportionally to the squared nuclear charge. Such a behavior of the cross section has a simple qualitative interpretation: With increasing nuclear charge the radius of the ground state of a hydrogen-like ion decreases $r_{1s} \propto Z^{-1}$, whence (on the assumption that $\sigma_{1s} \propto r_{1s}^2$) there follows the threshold dependence of the photoionization cross section that can also be represented as $\sigma_{1s}^{\text{thres}} \propto 1/I_{1s}$. Hence, it follows that the threshold value of the photoeffect cross section for *ns*-states (with another principal quantum number n) can be represented as

$$\sigma_{ns}^{\text{thres}} = (I_{1s}/I_{ns})\sigma_{1s}^{\text{thres}}. \tag{3.126}$$

Thus, the threshold value of the photoionization cross section increases with principal quantum number. Curiously, this relation is validated by experimental cross sections even in the case of non-hydrogen-like atoms. For example, for an argon atom we have $I_{1s} : I_{2s} : I_{3s} \approx 150 : 10 : 1$, while the ratio of experimental threshold cross sections for these shells is $300 : 30 : 1$.

In the high-frequency mode $\hbar\omega \gg I_{1s}$ we obtain from (3.124)

$$\sigma_{1s}(\omega) \approx \frac{2^8\pi}{3}\frac{a_B^2}{Z^2 137}\left(\frac{I_{1s}}{\hbar\omega}\right)^{7/2}\left[1 - \pi\sqrt{\frac{I_{1s}}{\hbar\omega}}\right]. \tag{3.127}$$

The formula (3.127) reflects the well-known asymptotic decrease in the hydrogen-like photoeffect cross section with increasing frequency: $\omega^{-7/2}$. It makes sense to emphasize that the photoionization cross section (3.124) goes to its asymptotic behavior (3.127) only at rather high values of frequency, i.e. about $\omega > 40I_{1s}/\hbar$ since the expansion parameter $(-2\pi\zeta)$ of the exponent in (3.124) becomes much less than unity only at such high frequencies.

For the photoionization of *nl*-subshells (with $l \neq 0$), the photoeffect cross section decreases also monotonically with increasing frequency, and for $\omega \gg I_{nl}/\hbar$ we have

$$\sigma_{nl}(\omega) \propto 1/\omega^{l+7/2}, \tag{3.128}$$

that is, the cross section decrease is more rapid.

As discussed above in relation with the Sommerfeld formula (3.124), there follow characteristic features for the cross sections of photoionization of a hydrogen-like ion, i.e. a maximum at threshold, a monotonic decrease with increasing frequency. These characteristic features, when going to multielectron atoms, are, generally speaking, violated. Nevertheless, the hydrogen-like formula for the photoionization cross section is a starting point for construction of an

approximate method of description by an order of magnitude. For example, if the high-frequency dependence (3.128) is employed from the threshold and combined with the sum rule $\frac{137}{2\pi^2 a_B \upsilon_a}\int_{I_{nl}}^{\infty}\sigma_{nl}(\omega)d\omega = N_{nl}$, we obtain the following photoionization cross section in the hydrogen-like approximation:

$$\sigma_{nl}(\omega) = \frac{4\pi^2 a_B^2}{137} N_{nl}\left(\frac{5}{2}+l\right)\frac{I_{nl}^{5/2+l}Ry}{(\hbar\omega)^{7/2+l}}. \tag{3.129}$$

The cross section (3.129) applied for the 1 s-electron gives a 3.2-fold excess over the exact value near the threshold, and far from the threshold an underestimation of 2.7 times. Therefore, (3.129) defines the cross section within an order of magnitude (in the hydrogen-like approximation).

For semiquantitative characterization of radiative phenomena, simple formulas obtained by Kramers within the framework of classical physics are often used. They describe cross sections for radiative processes in electron scattering in the field of a point charge. These formulas are valid for non-small values of the Born parameter $\zeta = Ze^2/\hbar\upsilon \geq 1$, that is, for large charge numbers and low electron velocities. In this case, the electron motion is quasi-classical and can be described to a good degree of accuracy as a motion along a classical trajectory.

Within the framework of the Kramers approach for the cross section of photoionization of an atomic subshell with quantum numbers nl, the following expression can be obtained (see Sect. 3.3):

$$\sigma_{nl}^{(Kr)}(\omega) = \frac{64\pi}{3\sqrt{3}} N_{nl}\frac{a_B^2}{137Z^2}\sqrt{\frac{Ry}{I_{nl}}}\left(\frac{I_{nl}}{\hbar\omega}\right)^3. \tag{3.130}$$

Hence, the formula (3.130) corresponds to the cross section of photoionization of a hydrogen atom in the ground state if it is assumed that $Z = N_{nl} = 1$ and $I_{nl} = Ry$. Figure 3.5 presents these results (dashed line) that demonstrate that, despite its simplicity, the Kramers formula adequately describes the cross section of photoionization of a hydrogen atom. The most distinction from the exact cross section is at threshold. The Kramers formula overestimates the Sommerfeld threshold value of the cross section by about 30%. In the high-frequency mode, the expression (3.130) gives another asymptotics than the Sommerfeld formula (3.124): ω^{-3} instead of $\omega^{-3.5}$. However, since the cross section goes to the high-frequency asymptotics only very far from the threshold (more than ten times), this distinction has little effect in the actual region of photon energies where the cross section is high.

3.7.3 Photoeffect Cross Section in the Born Approximation

In the mode of small values of the Born parameter $\zeta = Ze^2/\hbar v \ll 1$, the influence of an atomic core on the motion of an ionized electron can be considered to be a small perturbation. This is the case for high velocities and low nuclear charges. In this case, in calculation of the matrix elements $d_{\mathrm{nl},\varepsilon l+1}$ appearing in the general formula for the photoeffect cross section (3.122), plane waves corresponding to free motion can be used as a wave function of an ionized electron. Then for the cross section of photoionization of an atomic subshell, the following expression can be obtained:

$$\sigma_{\mathrm{nl}}(\omega) = \frac{8\pi^2}{3\cdot 137} N_{\mathrm{nl}} a_{\mathrm{B}}^2 \frac{Ry}{\hbar\omega} \left(\frac{p(\omega)}{\hbar}\right)^3 \left| g_{\mathrm{nl}}\left(\frac{p(\omega)}{\hbar}\right)\right|^2, \tag{3.131}$$

where $p(\omega) = \sqrt{2m(\hbar\omega - I_{\mathrm{nl}})}$ is the momentum of the ionized electron, I_{nl} is the potential of ionization of an electron subshell, $g_{\mathrm{nl}}(k) = \sqrt{\frac{2}{\pi}} \int_0^\infty j_l(kr) R_{\mathrm{nl}}(r) r^2 \mathrm{d}r$ is the Fourier transform of the radial wave function of the initial state of an atom, $R_{\mathrm{nl}}(r)$ is the radial wave function of the initial state of an atomic electron normalized according to $\int_0^\infty |R_{\mathrm{nl}}(r)|^2 r^2 \mathrm{d}r = 1$, and $j_l(kr)$ is the spherical Bessel function of the lth order.

Let us give for reference several spherical Bessel functions: $j_0(x) = \sin x/x$, $j_1(x) = \sin x/x^2 - \cos x/x$, $j_2(x) = (3x^{-3} - x^{-1})\sin x - 3\cos x/x^2$. Spherical Bessel functions describe the radial dependence of a spherical wave with a specified value of an orbital quantum number l.

In case of photoionization of the ground state of a hydrogen atom, we have: $R_{10}(r) = \left(2/\sqrt{a_{\mathrm{B}}^3}\right)\exp(-r/a_{\mathrm{B}})$ and $g_{10}(k) = \sqrt{\frac{2}{\pi}} \frac{4a_{\mathrm{B}}^{3/2}}{(1+k^2a_{\mathrm{B}}^2)^2}$, $N_{\mathrm{nl}} = 1$, $I_{\mathrm{nl}} = Ry$. Substituting these equations in the formula (3.131), we find the following expression for the cross section of photoionization of a hydrogen atom in the Born approximation:

$$\sigma_{1\mathrm{s}}^{(B)}(\omega) = \frac{2^8\pi}{3\cdot 137} a_{\mathrm{B}}^2 \frac{Ry}{\hbar\omega} \frac{(p(\omega)a_{\mathrm{B}}/\hbar)^3}{\left[1 + (p(\omega)a_{\mathrm{B}}/\hbar)^2\right]^4}. \tag{3.132}$$

The plot of the function $\sigma_{1\mathrm{s}}^{(B)}(\omega)$ is presented in Fig. 3.5 as a dashed-dotted line.

From Fig. 3.5 a characteristic feature of the Born cross section is seen: It goes to zero at the threshold in contrast to the exact Sommerfeld cross section and the approximate Kramers cross sections that have a maximum at the threshold. This is connected with the fact that the Born approximation does not take into account nuclear attraction that increases the cross section value. At the same time, the function (3.132) has correct high-frequency asymptotics $\sigma_{1\mathrm{s}}^{(B)}(\hbar\omega \gg Ry) \propto \omega^{-7/2}$

since in the mode of high photon energies an ionized electron can be considered to be free, which corresponds to the condition of applicability of the Born approximation. Nevertheless, the ratio of the Born cross section to the exact cross section for $\hbar\omega = 100$ eV is 2.1, at $\hbar\omega = 1$ keV it is 1.38, and only for $\hbar\omega = 10$ keV, this ratio is equal to 1.12; that is, the convergence is rather slow.

Thus for not too high photon energies the Kramers photoeffect cross section for a hydrogen atom describes the real situation better than the Born cross section.

3.7.4 Local Plasma Frequency Model

So far the photoionization cross section was calculated with neglect of interelectron interaction; that is, it was assumed that photon absorption occurs as a result of interaction of an electromagnetic field with individual electrons, the contributions of which are additively summed, giving the total cross section. There is a rather simple alternative approach to the description of an atomic photoeffect based on purely classical considerations. It is the *local plasma frequency model* or the Brandt–Lundqvist approximation (Brandt and Lundqvist 1965) that was considered in Sect. 2.6. Within the framework of this approach, an atom is approximated by an inhomogeneous distribution of electron density with concentration $n(r)$ (plus nucleus) [Rosmej et al. 2020]. Each spatial point corresponds to its own local plasma frequency $\omega_p(r) = \sqrt{4\pi e^2 n(r)/m}$, and interaction of an external electromagnetic field of frequency ω with atomic electrons is defined by the plasma resonance condition

$$\omega = \omega_p(r) = \sqrt{\frac{4\pi e^2 n(r)}{m}}. \tag{3.133}$$

From this equation, it follows that absorption of electromagnetic field energy by atomic electrons occurs at those distances from a nucleus where the local plasma frequency coincides with the ionizing radiation frequency. This model results in the following simple expression for the spectral function:

$$g(\omega) = \int d^3 r\, n(r)\, \delta\big(\omega - \omega_p(r)\big). \tag{3.134}$$

It is easy to see that the spectral function (3.134) satisfies the sum rule (3.118). For the photoionization cross section, according to (3.117), we have

$$\sigma(\omega) = \frac{2\pi^2}{137} a_B \upsilon_a \int d^3 r\, n(r)\, \delta\big(\omega - \omega_p(r)\big). \tag{3.135}$$

The presence of the delta function in (3.135) allows easy integration with respect to spatial variables. As a result, we obtain the so-called Brandt–Lundqvist approximation for the photoionization cross section:

$$\sigma_{\text{ph}}^{\text{B–L}}(\omega) = \frac{4\pi^2\omega}{137 v_a} r_\omega^2 \frac{n(r_\omega)}{|n'(r_\omega)|}, \tag{3.136}$$

where r_ω is the solution of (3.133). This value corresponds to the radial distance (from the nucleus) of the plasma resonance, and the prime denotes differentiation with respect to the radius. Thus, within the framework of the model, the photoeffect cross section is defined only by the distribution of the electron density $n(r)$. For the last value, it is convenient to use the statistical model of an atom, in which $n(r) = \left(Z^2/a_{\text{B}}^3\right) f(x = r/r_{\text{TF}})$, where $f(x)$ is the universal function of the reduced distance $x = r/r_{\text{TF}}$, Z is the nuclear charge, $r_{\text{TF}} = b a_{\text{B}} / Z^{1/3}$ is the Thomas–Fermi radius, and $b \cong 0.8853$. Substituting the above expression for electron density in the formula (3.136), we find

$$\sigma_{\text{ph}}^{\text{B–L}}(\omega) = s\left(v = \frac{\hbar\omega}{2Z\,Ry}\right) = \frac{9\pi^4 v}{32 \cdot 137} x_v^2 \frac{f(x_v)}{|f'(x_v)|} a_{\text{B}}^2, \tag{3.137}$$

here the reduced frequency $v = \hbar\omega/(2Z\,Ry)$ is introduced, and x_v is the solution of the equation $v = \sqrt{4\pi f(x)}$ being a result of (3.133).

As seen from (3.137), the photoionization cross section in the Brandt–Lundqvist approximation is found to be a universal function, that is, independent of nuclear charge but a function of the reduced frequency: $s(v)$. The formula (3.137) reveals a corresponding scaling law for the cross section with respect to the variable v. The universal function $s(v)$ is defined by the type of the statistical model of atom, that is, by the dependence of $f(x)$.

Figure 3.6 shows the calculation of the photoionization cross section of a krypton atom carried out within the framework of two alternative approaches: the quantum hydrogen-like approximation (3.129) (solid curve), and the classical local plasma model (3.137) that employs the Thomas–Fermi electron density (dotted curve).

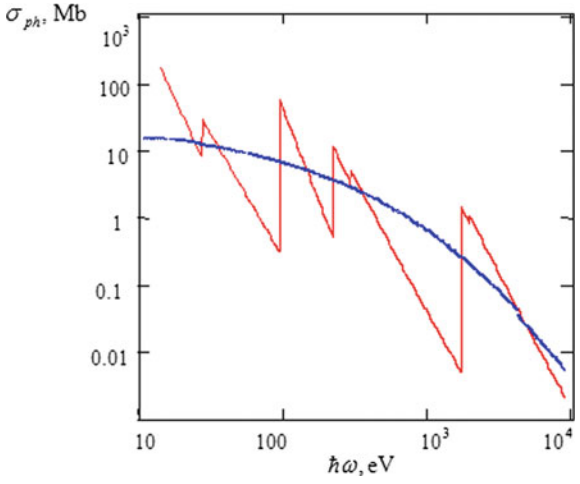

Fig. 3.6 Cross section of photoionization of a krypton atom: solid red curve—hydrogen-like approximation (3.129); dotted blue curve—local plasma model (3.137) with electron density according to the Thomas–Fermi model

It is seen that the first dependence is a saw-toothed curve with jumps at frequencies corresponding to the ionization potentials of electron subshells. The value of a jump decreases with increasing potential of subshell ionization according to the formula (3.126). The cross section of photoionization of an atom in the local plasma model (for the Thomas–Fermi electron density) is a smooth monotonically decreasing curve that describes in a smooth manner the quantum jumps of the hydrogen-like approximation.

The main advantages of the Brandt–Lundqvist approximation are simplicity, clearness, and universality. It gives the worst description of the process in spectral intervals in the vicinity of thresholds of ionization of electron subshells as it is seen from Fig. 3.6. In the original work of Brandt and Lundqvist (1965), it was noted that the local plasma model is adequate to physics of electromagnetic field photoabsorption by an atom not throughout the frequency range, but at frequencies $\omega \approx Z\,Ry/\hbar$ ($Ry = 13.6\,\mathrm{eV}$), when collective interactions dominate over one-particle interactions. For such frequencies, the distance to a nucleus, at which the plasma resonance condition (3.133) is satisfied (in the Thomas–Fermi model), coincides with the Thomas–Fermi radius, that is equal to the distance where the electron density is maximum. Therefore, the assumption of domination of collective phenomena in the photoeffect at frequencies $\omega \approx Z\,Ry/\hbar$ seems to be reasonable, at least at a qualitative level.

The use of the exponential screening model for the normalized function of the electron density $f(x = r/r_{\mathrm{TF}})$, i.e.

$$f_{\exp}(x) = \frac{128}{9\pi^3}\,e^{-2x} \tag{3.138}$$

allows obtaining a simple analytical expression for the photoeffect cross section. In this case, then the transcendental (3.133) is easily solved, and we obtain with the use of (3.137)

$$\sigma_{\mathrm{ph}}^{\mathrm{B-L(exp)}}(\omega = (2Z\,Ry/\hbar)v) = \frac{9\pi^4 a_{\mathrm{B}}^2 v}{64\cdot 137}\ln^2\left(\frac{16\sqrt{2}}{3\pi v}\right); \quad v \le \frac{16\sqrt{2}}{3\pi} \cong 2.4. \tag{3.139}$$

A characteristic feature of the cross section (3.139) is the existence of a "cutoff frequency", which is connected with limited radial electron density near a nucleus in the model (3.138). Therefore, there exists a radiation frequency, for which the plasma resonance condition is not satisfied. Another characteristic feature of the photoeffect cross section calculated with the function (3.138) is the presence of a pronounced maximum at $\hbar\omega_{\max}^{(\exp)} \cong 8.8Z$ eV.

The atomic photoeffect cross section calculated within the framework of the Brandt–Lundqvist approximation (3.137) while employing different statistical atomic models is presented in Fig. 3.7. We note, that the comparison of the local plasma frequency approach employing various atomic models shows often surprisingly good agreement with experimental photoionization cross section data (Rosmej et al. 2020).

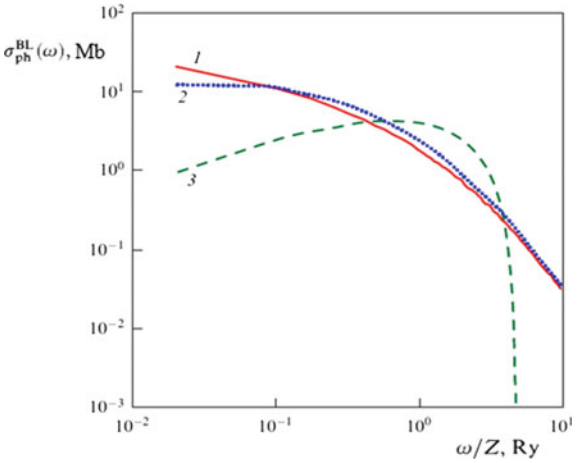

Fig. 3.7 Photoeffect cross section in the Brandt–Lundqvist approximation employing different statistical atomic models: 1—Thomas–Fermi, 2—Lenz–Jensen, 3—exponential screening

3.7.5 *Approximate Quantum Methods of Calculation of Photoabsorption Cross Sections*

Along with the above classical method of consideration of interparticle correlations in photoabsorption, there are approximate quantum methods taking into account multiparticle effects, in which the photoionization cross section is calculated with the use of somewhat more simplified approaches in comparison with consistent quantum mechanical consideration, such as the *random phase exchange approximation* (RPEA).

One of such methods is based on the *local electron density functional* (DFT) formalism. The simplification of calculation is achieved due to introduction of a local effective potential for the determination of one-particle wave functions of the ground state of a system. For this purpose, a *non-local* exchange-correlation energy is calculated in the local density approximation according to the equations

$$V_{xc}(r) = -\frac{0.611e^2}{r_s(r)} - \frac{0.1e^2}{3a_B}\ln\left(1 + \frac{11.4a_B}{r_s(r)}\right); \quad \frac{4}{3}\pi r_s^3(r) = n^{-1}(r). \qquad (3.140)$$

Equation (3.140) is the so-called exchange-correlation potential. As a result, the solutions of the corresponding equations are found to be no more difficult than the solution of the Hartree differential equations. The effects of interelectron interaction are taken into account with the use of the introduction of a self-consistent field representing the sum of external and induced fields and being a solution of an integral equation.

The results of such calculations are in excellent agreement with available experimental data. Besides, they are indicative of an important role of multiparticle effects in photoionization of atoms with filled electron shells. These effects result (except for the case of neon) in a considerable shift of the photoionization cross section maximum to

the region of higher frequencies in comparison with the independent electron approximation, when the position of a maximum practically coincides with the threshold energy of a photon. For example, the maximum of the cross section of photoionization of a xenon atom in the vicinity of the $4d$-threshold is shifted by about 2.5 Ry in the direction of high frequencies. In this case, there is no strong resonance connected (within the framework of one-particle consideration) with transition from the $4d$-subshell to the virtual f-state located in the continuous spectrum.

It is interesting to note that the local DFT method predicts a lower (by several electron-volts) value of the photoeffect threshold in comparison with its observed value. At the same time, this method does not describe highly excited states of the discrete spectrum of an atom. It should be emphasized that in this case the sum rule for the photoabsorption cross section is fulfilled because the "non-physical" contribution of the continuous spectrum to the cross section is compensated by the contribution of the discrete spectrum adjacent to the photoionization threshold that is not taken into account. This fact is present in a much more pronounced form in the above versions of classical description of the atomic photoeffect. As can be seen from Fig. 3.6, the Thomas–Fermi model for the atomic electron density gives a photoionization cross section that is strongly pulled into the low-frequency region, though the sum rule for corresponding cross sections is fulfilled. Within the framework of statistical models, naturally, there is no discrete energy spectrum of an atom at all, so the "non-physical" region of the continuous spectrum below photoionization threshold simulates to a certain extent the contribution of bound states not taken into account.

3.7.6 Rost Hybrid Method

Let us consider a simple model of an atomic photoeffect that admits the analytical representation of the process cross section, known as the Rost hybrid method (Rost 1995). From the formal point of view, this approach is based on the approximate operator equation:

$$\exp\left\{-\frac{i\left(\hat{H}_0+\Delta_1\right)t}{\hbar}\right\}\exp\left\{\frac{i\hat{H}_0 t}{\hbar}\right\}\approx\exp\left(-\frac{i\Delta_1 t}{\hbar}\right),\quad \Delta_1=\frac{e^2 a_{\mathrm{B}}}{r^2}, \tag{3.141}$$

where H_0 is the unperturbed Hamiltonian of the atom. Hence, the expression for the cross section is given by

$$\sigma_{\mathrm{ph}}(\omega)\approx\frac{2\pi Z^2 \upsilon_a^2}{3\cdot 137\omega}\int\limits_{-\infty}^{+\infty}\mathrm{d}t\langle\psi|\exp(-i\Delta_1 t/\hbar)|\psi\rangle e^{\mathrm{i}\omega t} \tag{3.142}$$

The representation of the cross section via (3.142) is called the "hybrid" approximation: It is quantum mechanically due to the general operator approach and at the same time has classical features since the approximate commutation of operator exponents (3.141) is used. It should be noted that the formula (3.142) can be rewritten in terms of the electron density if the following replacement is made:

$$|\psi(\boldsymbol{r})|^2 \rightarrow 4\pi r^2 n(r). \tag{3.143}$$

After integration with respect to time, the remaining integral (due to the presence of the delta function) can be represented as

$$\sigma_{\mathrm{ph}}(\omega) = \frac{8\pi^3 Z^2}{3 \cdot 137} a_{\mathrm{B}}^5 \left(\frac{2Ry}{\hbar\omega}\right)^{7/2} n\left(r = \sqrt{\frac{a_{\mathrm{B}} \upsilon_{\mathrm{a}}}{\omega}}\right). \tag{3.144}$$

In particular, from (3.144) it follows the hydrogen-like high-frequency asymptotics of the photoionization cross section if $n(r \rightarrow 0) \rightarrow const$. The dependence (3.144) is presented in Fig. 3.5 as a dotted curve.

Thus, as in the Brandt–Lundqvist approximation, the photoeffect cross section in the Rost hybrid approximation is found to be an electron density functional. But in this case the characteristic distance of the radiative process r_ω is not defined by the plasma resonance condition (3.133), but by the difference of the atomic Hamiltonians H_l with orbital quantum numbers differing (according to the dipole selection rules) by one:

$$\hbar\omega = H_1(r) - H_0(r). \tag{3.145}$$

Equation (3.145) immediately follows from (3.141) in view of the energy conservation law. Based on (3.145), it is possible to give a physical interpretation of the Rost approximation. From this equation, it follows that photon absorption occurs with a fixed electron coordinate as in the Born–Oppenheimer approximation, where the values of coordinates of molecular nuclei do not change during an electron transition. It should be noted that the formula (3.141) is just a mathematical expression of this fact. So the Rost hybrid approximation can be considered as a generalization of the adiabatic principle to the case of electron transitions in atoms.

It should be emphasized that the Rost model does not fulfill the sum rule for the photoabsorption cross section (3.118) in contrast to the Brandt–Lundqvist approximation. This hints to the inconsistency of the hybrid approach used in the derivation of the expression for the photoeffect cross section within the framework of this model.

3.7.7 Generalized Scaled Empirical Photoionization Cross Sections from K-, L-, M-, N- and O-Shell

Quantum mechanical numerical calculations for the photoionization cross sections of different subshells have been performed in a Z- and energy threshold-scaled representation that allow to establish a generalised scaled photoionization model GSPM (Rosmej et al. 2020):

$$\sigma^{(\mathrm{phi})} = \frac{\pi a_0^2}{Z_{\mathrm{eff}}^2} \cdot \frac{m}{2l_0+1} \cdot P_1 \cdot \frac{u+P_2}{u+P_3} \cdot \frac{1}{(u+P_4)^{7/2+l_0}}, \tag{3.146a}$$

$$u = \frac{E - E_{\mathrm{n}_0 l_0}}{\tilde{Z}^2 \cdot Ry}, \tag{3.146b}$$

$$Z_{\mathrm{eff}} = n_0 \sqrt{\frac{E_{\mathrm{n}_0 l_0}}{Ry}}, \tag{3.146c}$$

$$\tilde{Z} = Z_{\mathrm{eff}} + (Z_{\mathrm{eff}} - z) \qquad \text{for single electrons in outer shell } n_0 l_0, \tag{3.146d}$$

$$\tilde{Z} = Z_{\mathrm{n}} - N_{\mathrm{bound}} + N_{\mathrm{nl} \geq n_0 l_0} \qquad \text{for inner-shell ionization.} \tag{3.146e}$$

a_0 is the Bohr radius ($\pi a_0^2 = 8.79 \times 10^{-17}\mathrm{cm}^2$), m is the number of equivalent electrons in the subshell $n_0 l_0$, n_0 and l_0 are principal and orbital quantum number, respectively, Ry = 13.606 eV, Z_n is the nuclear charge, $E_{\mathrm{n}_0 l_0}$ is the ionization potential, N_{bound} is the number of bound electrons, $z = Z_{\mathrm{n}} - N_{\mathrm{bound}} + 1$ is the spectroscopic symbol, $N_{\mathrm{nl} \geq n_0 l_0}$ is the number of electrons in subshells higher or equal than

Table 3.3 Numerical quantum mechanical calculations of the photoionization cross section from H-like ions from the $n_0 l_0$-subshells

$n_0 l_0$	P_1	P_2	P_3	P_4
1s	4.667×10^{-1}	2.724×10^{0}	9.458×10^{0}	1.189×10^{0}
2s	5.711×10^{-2}	6.861×10^{-1}	7.768×10^{0}	3.644×10^{-1}
2p	8.261×10^{-2}	1.843×10^{-1}	7.340×10^{0}	2.580×10^{-1}
3s	1.682×10^{-2}	1.436×10^{-1}	7.356×10^{0}	1.436×10^{-1}
3p	2.751×10^{-2}	1.742×10^{-1}	7.162×10^{0}	1.742×10^{-1}
3d	3.788×10^{-3}	1.566×10^{-1}	7.880×10^{0}	1.566×10^{-1}
4s	7.096×10^{-3}	8.799×10^{-2}	7.308×10^{0}	8.799×10^{-2}
4p	1.493×10^{-2}	1.197×10^{-1}	1.027×10^{1}	1.197×10^{-1}
4d	1.769×10^{-3}	1.205×10^{-1}	6.346×10^{0}	1.205×10^{-1}
4f	1.092×10^{-4}	1.055×10^{-1}	9.231×10^{0}	1.055×10^{-1}
5s	3.956×10^{-3}	5.846×10^{-2}	8.651×10^{0}	5.846×10^{-2}

For H-like ions, $\tilde{Z} = Z_{\mathrm{eff}} = Z_{\mathrm{n}}$. Fitting parameters are generally accurate within 20% in the large energy range from $10^{-3} < u < 32$(i.e., from threshold to about 30 times threshold)

the subshell $n_0 l_0$, and P_1, P_2, P_3, P_4 are fitting parameters that are given in Table 3.3. The scaled formula (3.146) provides a precision of about 20% of the photoionization cross sections of H-like ions when employing the parameters given in Table 3.3. The particular advantage of the developed formula (3.146) is that it shows the right high-energy and low-energy asymptotics that have been discussed above.

Let us first consider the application of formulas (3.146) to the threshold value of hydrogen discussed above (Sect. 3.7.2). From (3.146) and the parameters for the $1s$ state in Table 3.1, it follows with $l_0 = 0$, $m = 1$, $Z_{\text{eff}} = 1$, $\sigma^{(\text{phi})}(1s) \approx 6.4 \times 10^{-20}\text{cm}^2$. This is in excellent agreement with the exact value of the Sommerfeld formula (3.124) that gives $\sigma^{(\text{phi})}(1s) = 6.3 \times 10^{-20}\text{cm}^2$.

Now, we consider photoionization from the $2p$-shell of H-like helium, i.e. the transition $2p + \hbar\omega \rightarrow \text{nuc} + e$ at a photon energy of 122 eV: $Z_{\text{eff}} = 2$, $u = 2$, $l_0 = 1$, $m = 1$ and the fitt-parameters for the $2p$ state in Table 3.1 it follows $\sigma^{(\text{phi})}(2p) \approx 3.7 \times 10^{-21}\text{cm}^2$ whereas the exact quantum mechanical numerical result is $\sigma^{(\text{phi})}(2p) = 3.7 \times 10^{-21}\text{cm}^2$.

The fitt-parameters might also be used to estimate the photoionization cross section for non-H-like ions in the framework of the H-like approximation with effective charges. Let us consider for demonstration of the application of (3.146) the photoionization from Li-like aluminum: (a) transition $1s^2 2s + \hbar\omega \rightarrow 1s^2 + e$ at a photon energy of 7020 eV: $E_{2s} \approx 442\,\text{eV}$ form which it follows $Z_{\text{eff}} \approx 11.4$. Because the considered $2s$-electron corresponds to the photoionization of a single outer electron $\tilde{Z} = 11.8$ and $u = 3.47$. With $l_0 = 0$ and $m = 1$ and the fitt-parameters for the $2s$ state in Table 3.1 it follows $\sigma_{\text{fit}}^{(\text{phi})}(2s) \approx 1.3 \times 10^{-22}\text{cm}^2$. The quantum mechanical numerical result is $\sigma^{(\text{phi})}(2s) = 1.3 \times 10^{-22}\text{cm}^2$, (b) transition $1s^2 3d + \hbar\omega \rightarrow 1s^2 + e$ at a photon energy of 1010 eV: $E_{3d} \approx 183\,\text{eV}$ form which it follows $Z_{\text{eff}} \approx 11.0$. Because the considered "d-electron" corresponds to the photoionization of a single outer electron $\tilde{Z} = Z_{\text{eff}}$ and $u = 0.5$. With $l_0 = 2$ and $m = 1$ and the fitt-parameters for the "d-state" in Table 3.1, it follows $\sigma_{\text{fit}}^{(\text{phi})}(3d) \approx 4.3 \times 10^{-22}\text{cm}^2$. The quantum mechanical numerical result is $\sigma^{(\text{phi})}(3d) = 4.4 \times 10^{-22}\text{cm}^2$, (c) let us consider a more complicated ground state, the transition $1s^2 2s^2 2p^2 + \hbar\omega \rightarrow 1s^2 2s^2 2p^1 + e$ in B-like neon at a photon energy of 2117 eV: $E_{2p} \approx 158\text{eV}$ from which it follows $Z_{\text{eff}} \approx 6.81$, $\tilde{Z} = 7.62$ and $u \approx 2.48$. With $l_0 = 1$ and $m = 2$ and the fitt-parameters for the 2p state in Table 3.1, it follows $\sigma^{(\text{phi})}(2p) \approx 1.5 \times 10^{-22}\text{cm}^2$. The quantum mechanical numerical result is $\sigma^{(\text{phi})}(2p) = 2.3 \times 10^{-22}\text{cm}^2$. These examples have general character: The H-like approximation is valid for excited states, whereas for ground and close to ground state excited states, specific numerical calculations are requested and in these cases (3.146) might be used only for an order of magnitude estimate.

We now apply the parameters of Table 3.1 to non-hydrogen-like ions and inner-shell photoionization (of primary interest for X-ray Free Electron Laser applications) with the help of the rescaling relation (3.146b, e). We consider the photoionization of the $1s$- and $2s$-shells of B-like Neon at a photon energy of

2000 eV: (a) the ionization potential for the transition $1s^2 2s^2 2p^1 + \hbar\omega \rightarrow 1s^1 2s^2 2p^1 + e$ is $E_{1s} \approx 1050\,\text{eV}$ from which it follows $Z_{\text{eff}} \approx 8.78$. Because the ionization of the $1s$-electron corresponds to inner-shell ionization, $Z_{\text{n}} = 10$, $N_{\text{bound}} = 5$, $N_{\text{nl} \geq n_0 l_0}(1s) = 5$ and $\tilde{Z} = 10 - 5 + 5 = 10$ from which it follows $u = 0.70$. With $l_0 = 0$ and $m = 2$ and the fitt-parameters for the $1s$ state in Table 3.1, it follows $\sigma^{(\text{phi})}(1s) \approx 3.8 \times 10^{-20}\text{cm}^2$. The quantum mechanical numerical result is $\sigma^{(\text{phi})}(1s) = 3.9 \times 10^{-20}\text{cm}^2$; (b) we now consider the transition $1s^2 2s^2 2p^1 + \hbar\omega \rightarrow 1s^2 2s^1 2p^1 + e$ for a photon energy of 2132 eV: $E_{2s} \approx 173\,\text{eV}$ from which it follows $Z_{\text{eff}} \approx 7.13, N_{\text{nl}} > n_0 l_0(2s) = 3$, $\tilde{Z} = 10 - 5 + 3 = 8$ and $u \approx 2.10$. With $l_0 = 0$, $m = 2$ and the fitt-parameters for the $2s$ state in Table 3.1 it follows $\sigma^{(\text{phi})}(2s) \approx 2.0 \times 10^{-21}\text{cm}^2$. The quantum mechanical numerical result is $\sigma^{(\text{phi})}(2s) = 2.3 \times 10^{-21}\text{cm}^2$. The general precision for inner-shell photoionization is difficult to estimate, but (3.146) might estimate inner-shell photoionization cross sections within a factor of 2 or so but might be only an order of magnitude estimate in more complex cases (Rosmej et al. 2020).

3.8 Photodetachment from Negative Ions

Several atoms and molecules, having captured an electron, can form negative ions. As a result of such a capture, energy is released that is called electron affinity energy. In Table 3.4, the electron affinity energy ε_{a} is given for a number of atoms and molecules.

An affinity energy means that energy is necessary to move an outer electron from the negative ion to infinity. This energy can be transferred to an ion as a result of absorption of a photon of sufficiently high frequency $\omega > \varepsilon_{\text{a}}/\hbar$. The process of detachment of an outer electron of a negative ion under the action of an electromagnetic field is called *photodestruction*. In case of photodestruction of a negative ion, a detached electron is in a neutral atom field that is much more weak than the long-range Coulomb field of an ion. So in the first approximation, it is possible to neglect the influence of an atom on a detached electron, assuming it to be free, and to use a plane wave for its wave function. In other words, for description of photodestruction of a negative ion the Born approximation is adequate, so the formula (3.131) should be valid. The specific photodestruction cross section is then defined by the form of the functions $g_{\text{nl}}(k)$ representing the Fourier transform of a wave function of an outer electron of a negative ion. The simplest model that can be used for the radial wave function $R_{\text{nl}}(r)$ of a negative ion is called the zero radius

Table 3.4 Electron affinity energies

Ion	H	Li	O	F	S	Cl	O_2	H_2O
ε_{a}, eV	0.75	0.58	1.47	3.45	2.08	3.6	0.45	0.9

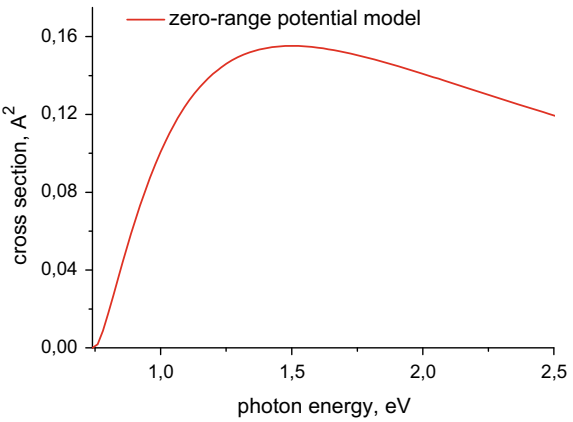

Fig. 3.8 Cross section of photodestruction of a negative ion of a hydrogen atom calculated in the zero radius potential approximation

potential approximation. In this approximation, we have: $R_{10}^{(0)}(r) = \sqrt{2\gamma}\exp(-\gamma r)/r$, where $\gamma = \sqrt{2m\varepsilon_a}/\hbar$ is the parameter of the reciprocal characteristic length of the potential. Using this wave function, we obtain from (3.131):

$$\sigma_{ph}^{(0)}(\omega) = \frac{4\pi}{3\cdot 137} a_B^2 \sqrt{\frac{\varepsilon_a}{Ry}} \left(\frac{\sqrt{2m(\hbar\omega - \varepsilon_a)}}{m a_B \omega} \right)^3 . \tag{3.147}$$

The spectral dependence of the cross section (3.147) is shown in Fig. 3.8.

It is seen that at threshold the cross section goes to zero as it should be in the Born approximation. The maximum of the spectral dependence is reached at a photon energy approximately equal to the double affinity energy of a hydrogen atom (0.75 eV). The value of the cross section itself at maximum is 2.6 times higher than the maximum cross section of photoionization of the neutral hydrogen.

From the formula (3.147), there follows the high-frequency asymptotics of the cross section of photodestruction of a negative hydrogen ion in the zero radius potential approximation: $\sigma_{ph}^{(0)}(\omega) \propto \omega^{-1.5}$, that is, with increasing frequency the cross section decreases much more slowly than in case of photoionization of neutral hydrogen.

The zero radius potential approximation is favorably distinguished by its simplicity but gives results differing essentially from those of more accurate models. Besides, in case of negative ions of atoms with high polarizability, in calculation of the photodestruction cross section it is necessary to take into account variable polarization of the atomic core that appreciably changes the cross section.

The polarization of a core can also play an essential role in the process of ionization of neutral multielectron atoms. This multiparticle effect at a quantum level is taken into account in the random phase exchange approximation, and within the framework of the classical picture, it is considered in the local plasma frequency approximation.

3.9 Phase Control of Photoprocesses by Ultrashort Laser Pulses

For ultrashort laser pulses, we have to consider the total probability W for the elementary atomic physics processes instead of the probability per unit time (Rosmej et al. 2014, 2016, 2021):

$$W = \frac{c}{4\pi^2}\int_0^\infty \sigma(\omega')\frac{|E(\omega',\tau)|^2}{\hbar\omega'}\mathrm{d}\omega', \tag{3.148}$$

where c – velocity of light, $E(\omega')$ – Fourier transform of electric field in the pulse, τ – pulse duration, and $\sigma(\omega')$ – cross section of the elementary process under consideration. Let us apply the so-called corrected Gaussian pulse to obtain explicit expressions for the probabilities for the photoexcitation. The Fourier transform of this pulse has the form (Rosmej et al. 2014):

$$E_{\mathrm{CGP}}(\omega',\omega,\tau,\varphi) = iE_0\tau\sqrt{\frac{\pi}{2}}\frac{\omega'^2\tau^2}{1+\omega^2\tau^2}\left\{e^{-i\varphi-(\omega-\omega')^2\tau^2/2} - e^{i\varphi-(\omega+\omega')^2\tau^2/2}\right\}, \tag{3.149}$$

where E_0, ω, and τ are the pulse amplitude, carrier frequency, and duration, respectively, and φ is the initial phase. An important feature of (3.149) is the absence of an electric field component at zero current frequency in contrast with the widely used expression of the standard Gaussian shape. Let us apply the formula (3.148) for calculation of the photoexcitation of a multielectron atom by an ultrashort Gaussian pulse (3.149) in the local plasma frequency model. Within the framework of this model, the expression for the photoabsorption cross section looks like

$$\sigma_{\mathrm{ph}}^{(\mathrm{BL})}(\omega') = \frac{2\pi^2e^2}{mc}\int n(r)\delta\big(\omega'-\omega_{\mathrm{pl}}(r)\big)\mathrm{d}\boldsymbol{r}, \tag{3.150}$$

where $\omega_{\mathrm{pl}}(r) = \sqrt{4\pi e^2 n(r)/m}$ is the local plasma frequency, and $n(r)$ is the spatial distribution of electron density in an atom. Substituting (3.150) in (3.148), we find

$$W_{\mathrm{tot}}^{(\mathrm{ph})} = \frac{\sqrt{\pi}e}{\sqrt{m}\hbar}\int_0^\infty \left|E\big(\omega_{\mathrm{pl}}(r),\varphi\big)\right|^2\sqrt{n(r)}r^2\mathrm{d}r, \tag{3.151}$$

where $\left|E\big(\omega_{\mathrm{pl}}(r),\varphi\big)\right|^2$ is the squared absolute value of the Fourier transform of the electric field calculated at the local plasma frequency, in which the carrier envelope phase dependence is clearly indicated. To analyze phase effects in the total

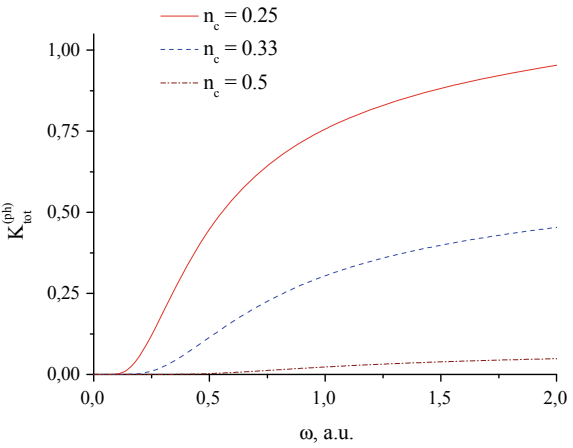

Fig. 3.9 Phase modulation factor for the total probability of photoabsorption of an ultrashort pulse by an atom as a function of carrier frequency

probability of photoexcitation by ultrashort laser pulses, we will introduce a phase modulation factor according to

$$K_{\text{tot}}^{(\text{ph})} = 2\frac{W_{\text{tot}}^{(\text{ph})}(\varphi = 0) - W_{\text{tot}}^{(\text{ph})}(\varphi = \pi/2)}{W_{\text{tot}}^{(\text{ph})}(\varphi = 0) + W_{\text{tot}}^{(\text{ph})}(\varphi = \pi/2)}. \tag{3.152}$$

The phase modulation factor for the total probability of photoabsorption by an atom with the charge $Z = 30$ calculated within the framework of the statistical model for electron density is presented in Fig. 3.9 for three pulse durations as a function of carrier frequency. The dimensionless parameter n_c is the number of periods in the radiation pulse at given carrier frequency.

It is seen that an appreciable dependence of the photoabsorption probability on the carrier envelope phase exists only for $n_c < 0.5$. The phase modulation factor for the fixed parameter n_c increases with carrier frequency. It should be noted that the photoabsorption probability at the high-frequency boundary of Fig. 3.9 is 15% of its maximum value (that in this model corresponds to the frequency $\omega_{\max} = 0.4$ a.u.).

The expression for the total photoabsorption probability (3.148) can be used to study the interaction of an ultrashort pulse with a *metal nanosphere* in a dielectric medium. If the radiation wavelength far exceeds the nanoparticle radius r_s, the dynamic polarizability of a nanoparticle can be described by the Lorentz formula:

$$\beta_s(\omega) = \frac{\varepsilon_s(\omega) - \varepsilon_m}{\varepsilon_s(\omega) + 2\varepsilon_m} r_s^3, \tag{3.153}$$

$\varepsilon_s(\omega)$ is the dielectric permittivity of a nanoparticle metal, and ε_m is the dielectric permittivity of the matrix. Hence, with the use of the optical theorem (2.52), it is possible to find the photoabsorption cross section in the dipole approximation and

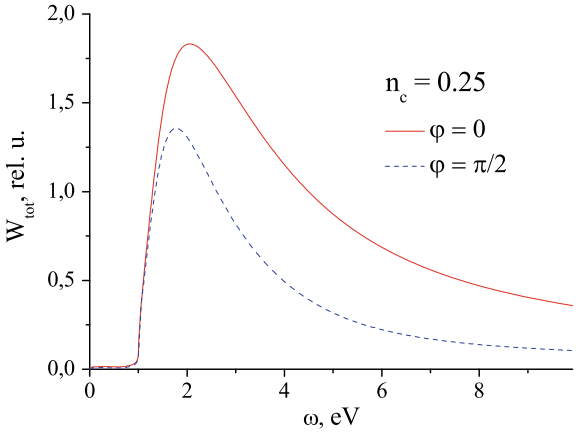

Fig. 3.10 Total probability of photoabsorption of an ultrashort pulse ($n_c = 0.25$) on a silver sphere ($r_s = 5.3$ nm) as a function of carrier frequency for two values of the carrier envelope phase

with the help of the formula (3.148) the total photoabsorption probability during the action of the pulse.

The photoabsorption probabilities of an ultrashort pulse by a silver nanoparticle in a glass matrix are given in Fig. 3.10 for two values of carrier envelope phase. The frequency dependence of the dielectric permittivity of silver is restored with the use of data on the real and imaginary parts of the refractive index.

It is seen that for the present case ($n_c = 0.25$) there is an essential dependence of photoabsorption on the carrier envelope phase, especially for photon energies at the carrier frequency exceeding the energy at the maximum. With increasing radiation pulse duration, the dependence of the probability on the carrier envelope phase becomes less appreciable and for $n_c > 0.5$ practically disappears (see Fig. 3.9).

In a number of cases, for excitation of a quantum system a sequence of identical pulses separated by a time interval T (not to be confused with the oscillation period designation) is used. It is not difficult to obtain the Fourier transform of the electric field strength for such a sequence consisting of N identical pulses in terms of the Fourier transform of a single pulse $E(\omega)$:

$$E_N(\omega) = \frac{\sin(\omega TN/2)}{\sin(\omega T/2)} \exp\left[i\frac{(N-1)\omega T}{2}\right] E(\omega). \tag{3.154}$$

Substituting (3.154) in the right-hand side of the (3.148), we find the probability of photoexcitation of a quantum transition under the action of N identical pulses:

$$W_{21}(N) = \frac{c}{4\pi^2\hbar} \int \frac{\sigma_{21}(\omega)}{\omega} \left[\frac{\sin(\omega TN/2)}{\sin(\omega T/2)}\right]^2 |E(\omega)|^2 d\omega. \tag{3.155}$$

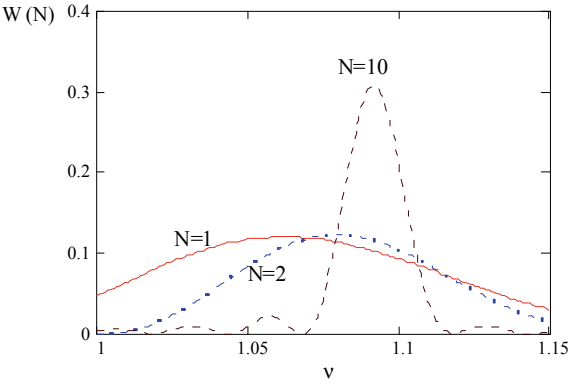

Fig. 3.11 Probability of H-atom photoionization by the action of a train of N two-cycle long laser pulses

Let us use these expressions for the description of the photoionization of a hydrogen atom under the action of a train of short pulses. In this case, the process cross section $\sigma_{21}(\omega)$ is given by the Sommerfeld formula that can be written as [see (3.124)]:

$$\sigma_{\mathrm{H}}\left(v=\frac{\hbar\omega}{Ry}\right)=\frac{2^9\pi^2 a_{\mathrm{B}}^2}{3\cdot 137\cdot v^4}\frac{\exp\left(-\dfrac{4arctg\sqrt{v-1}}{\sqrt{v-1}}\right)}{1-\exp\left(-2\pi/\sqrt{v-1}\right)}, \tag{3.156}$$

where $a_{\mathrm{B}}\cong 0.53$ Å is the Bohr radius, and $Ry\cong 13.6$ eV is the Rydberg constant.

The photoionization probabilities of a hydrogen atom due to the action of N laser pulses with duration equal to two cycles in dependence of the carrier frequency are presented in Fig. 3.11 [using formulas (3.155)–(3.156)]. The abscissa is expressed in terms of the dimensionless parameter $v=\varepsilon/Ry+1$, where $\varepsilon=\hbar\omega-Ry$ is the energy of ionized electron.

One can see from Fig. 3.11 that the spectral dependence of the photoionization probability shows a narrowing that increases with the number N of laser pulses. The value of the parameter ν at maximum is determined by the equation $\omega T=2\pi k$ (here k is a natural number). Since the energy of the ionized electron is equal to $Ry(v-1)$ and the number of these electrons is proportional to the probability $W(N)$, one can conclude that it is possible to manipulate considerably the energy spectrum of the photoelectron by changing the laser pulse parameters.

References

M.Y. Amusia, *Atomic Photoeffect* (Springer, Berlin, 1990)

D.R. Bates, A. Damgaard, The calculation of the absolute strengths of spectral lines. Phil. Trans. **242**, 101 (1949)

H.A. Bethe, E.E. Salpeter, *Quantum Mechanics of One- and Two Electron Atoms* (Springer, Berlin, 1977)

W. Brandt, S. Lundqvist, Atomic oscillations in the statistical approximation. Phys. Rev. **139**, A612 (1965)

R.D. Cowan, *The Theory of Atomic Structure and Spectra* (University of California Press, Berkeley, 1981)

V.A. Davydkin, B.A. Zon, Radiation and polarization characteristics of Rydberg atomic states. Opt. Spectrosk. **51**, 13 (1981)

R.A. Gantsev, N.F. Kazakova, V.P. Krainov, Radiation transition rates in hydrogen-like plasmas, in *Plasma Chemistry*, vol. 12, ed. by B.M. Smirnov (Energoatomizdat, Moscow, 1985), p. 96

H. Gao, D.R. DeWitt, R. Schuch, W. Zong, S. Asp, M. Pajek, Observation of enhanced electron-ion recombination rates at very low energies. Phys. Rev. Lett. **75**, 4381 (1995)

H. Gao, R. Schuch, W. Zong, E. Justinianoz, D.R. DeWitt, H. Lebius, W. Spies, Energy and charge dependence of the rate of electron–ion recombination in cold magnetized plasmas. J. Phys. B **30**, L499–L506 (1997)

V.I. Gervids, V.I. Kogan, Penetration and screening effects in electron bremsstrahlung on ions. JETP Lett. **22**, 142 (1975)

V.I. Gervids, V.I. Kogan, Electron bremsstrahlung in a static potential, in *Polarization Bremsstrahlung of Particles and Atoms*, eds. by V.N. Tsytovich, I.M. Oiringel (Plenum, New York, 1991)

S.P. Goreslavsky, N.B. Delone, V.P. Krainov, Probabilities of radiative transitions between highly excited atomic states. JETP **55**, 1032 (1982)

H.R. Griem, *Spectral Line Broadening by Plasmas* (Academic Press, New York, 1974)

H.R. Griem, *Principles of Plasma Spectroscopy* (Cambridge University Press, New York, 1997)

C. Heerlein, G. Zwicknagel, C. Toepffer, Radiative recombination enhancement of bare ions in storage rings with electron cooling. Phys. Rev. Lett. **89**, 83202 (2002) and erratum Phys. Rev. Lett. **93**, 209901(E) (2004a)

C. Heerlein, G. Zwicknagel, C. Toepffer, Reply to Hörndl et al. PRL **93**, 209301 (2004). Phys. Rev. Lett. **93**, 209302 (2004b)

A. Hoffknecht, C. Brandau, T. Bartsch, C. Böhme, H. Knopp, S. Schippers, A. Müller, C. Kozhuharov, K. Beckert, F. Bosch, B. Franzke, A. Krämer, P.H. Mokler, F. Nolden, M. Steck, Th Stöhlker, Z. Stachura, Recombination of bare Bi83+ ions with electron. Phys. Rev. A **63**, 012702 (2001)

M. Hörndl, S. Yoshida, K. Tokési, J. Burgdörfer, Comment on radiative recombination enhancement of bare ions in storage rings with electron cooling. Phys. Rev. Lett. **93**, 209301 (2004)

M. Hörndl, S. Yoshida, A. Wolf, G. Gwinner, J. Burgdörfer, Enhancement of low energy electron-ion recombination in a magnetic field: Influence of transient field effects. Phys. Rev. Lett. **95**, 243201 (2005)

J. Jackson, *Classical Electrodynamics*, 3rd edn. (Wiley, New York, 2007)

L. Kim, R.H. Pratt, Direct radiative recombination of electrons with atomic ions: cross sections and rate coefficients, Phys. Rev. A **27**, 2913 (1983)

V.I. Kogan, A.B. Kukushkin, Radiation emission by quasiclassical electrons in an atomic potential. JETP **60**, 665 (1984)

V.I. Kogan, A.B. Kukushkin, V.S. Lisitsa, Kramers electrodynamics and electron-atomic radiative-collisional processes. Phys. Rep. **213**, 1 (1992)

H.A. Kramers, On the theory of X-ray absorption and of the continuous X-ray spectrum. Phil. Mag. **46**, 836 (1923)

A.B. Kukushkin, V.S. Lisitsa, Radiative cascades between Rydberg atomic states. JETP **61**, 937 (1985)

L.D. Landau, E.M. Lifschitz, *Quantum Mechanics: Nonrelativistic Theory* (Pergamon, Oxford, 1977)

L.D. Landau, E.M. Lifschitz, *The Classical Theory of Fields* (Pergamon, Oxford, 2003)

L.D. Landau, E.M. Lifschitz, *Mechanics* (Pergamon, Oxford, 2005)

P.F. Naccache, Matrix elements and correspondence principles. J. Phys. B: At. Mol. Opt. Phys. **5**, 1308 (1972)

F.B. Rosmej, V.A. Astapenko, V.S. Lisitsa, Effects of ultrashort laser pulse durations on Fano resonances in atomic spectra. Phys. Rev. A **90**, 043421 (2014)
F.B. Rosmej, V.A. Astapenko, V.S. Lisitsa, Scaling laws for ionization of atomic states by ultra-short electromagnetic pulses. J. Phys. B **49**, 025602 (2016)
F.B. Rosmej, V.A. Astapenko, V.S. Lisitsa, XUV and X-ray elastic scattering of attosecond electromagnetic pulses on atoms. J. Phys. B: At. Mol. Opt. Phys. **50**, 235601 (2017)
F.B. Rosmej, V.A. Vainshtein, V.A. Astapenko, V.S. Lisitsa, *Statistical and quantum photoionization cross sections in plasmas: analytical approaches for any configurations including inner shells*, Matter and Radiation at Extremes (Review) **5**, 064202 (2020). Open access: https://aip.scitation.org/doi/10.1063/5.0022751
F.B. Rosmej, V.A. Astapenko, E. Khramov, *XFEL and HHG interaction with matter: effects of ultrashort pulses and random spikes*, Letter to Matter and Radiation at Extremes **6**, 034001 (2021).Open access: https://doi.org/10.1063/5.0046040
F.B. Rosmej, V.A. Vainshtein, V.A. Astapenko, V.S. Lisitsa, *Semi-empirical analytical radiative recombination rates into nl = 1s−9l states for hydrogen and non H-like ions*, in preparation for Matter and Radiation at Extremes (2022)
J.M. Rost, Analytical total photo cross section for atoms. J. Phys. B. **28**, L601 (1995)
I.I. Sobelman, *Introduction to the Theory of Atomic Spectra* (Pergamon, Oxford, 1972)
I.I. Sobelman, *Theory of Atomic Spectra* (Alpha Science Int. Limited, Oxford, UK, 2006)
I.I. Sobelman, L.A. Vainshtein, E.A. Yukov, *Excitation of Atoms and Broadening of Spectral Lines*, 2nd edn. (Springer, Berlin, 1995)
A. Sommerfeld, *Atombau and Spektrallinien: Band I und II* (Harri Deutsch, Frankfurt, 1978)
A. Unsöld, *Physik der Sternatmosphären* (Springer, Berlin, 1955)